Received: 25 December 2015 | Revised: 2 October 2017 | Accepted: 10 October 2017

DOI: 10.1111/iar.12243

WILEY Island Arc

RESEARCH ARTICLE

Depositional ages and characteristics of Middle–Upper Jurassic and Lower Cretaceous lacustrine deposits in southeastern Mongolia

Hitoshi Hasegawa[1,2] | Hisao Ando[3] | Noriko Hasebe[4] | Niiden Ichinnorov[5] | Tohru Ohta[6] | Takashi Hasegawa[7] | Masanobu Yamamoto[8] | Gang Li[9] | Bat-Orshikh Erdenetsogt[10] | Ulrich Heimhofer[11] | Takayuki Murata[3] | Hironori Shinya[6] | G. Enerel[12] | G. Oyunjargal[12] | O. Munkhtsetseg[12] | Noriyuki Suzuki[13] | Tomohisa Irino[8] | Koshi Yamamoto[14]

[1]Department of Global Environment and Disaster Prevention, Faculty of Science and Technology, Kochi University, Kochi 780-8520, Japan

[2]University Museum, Nagoya University, Furo-cho, Chikusa-ku, Nagoya 464-8601, Japan

[3]Department of Earth Sciences, Faculty of Science, Ibaraki University, Bunkyo, Mito 310-8512, Japan

[4]Institute of Nature and Environmental Technology, Kanazawa University, Kakuma, Kanazawa 920-1192, Japan

[5]Institute of Paleontology and Geology, Mongolian Academy of Sciences, P.O.B. 260, Ulaanbaatar 210351, Mongolia

[6]Department of Earth Sciences, Faculty of Education and Integrated Arts and Sciences, Waseda University, Nishiwaseda, Shinjuku, Tokyo 169-8050, Japan

[7]Department of Earth Sciences, Faculty of Science, Kanazawa University, Kakuma, Kanazawa 920-1192, Japan

[8]Faculty of Environmental Earth Science, Hokkaido University, Kita 8, Nishi 5, Kita-ku, Sapporo 060-0810, Japan

[9]Nanjing Institute of Geology and Palaeontology, Chinese Academy of Science, 39 East Beijing Road, Nanjing 210008, China

[10]Department of Geology and Geophysics, National University of Mongolia, KH Surguuliin Gudamj-1, Ulaanbaatar 14200, Mongolia

[11]Institute for Geology, Leibniz University Hannover, Welfengarten 1, Hannover D-30167, Germany

[12]School of Geology and Mining, Mongolian University of Science and Technology, Baga

Abstract

Lower Cretaceous lacustrine oil shales are widely distributed in southeastern Mongolia. Due to the high organic carbon content of oil shale, many geochemical studies and petroleum exploration have been conducted. Although most of the oil shales are considered to be Early Cretaceous in age, a recent study reveals that some were deposited in the Middle Jurassic. The present study aims at establishing depositional ages and characteristics of the Jurassic and Cretaceous lacustrine deposits in Mongolia. The Lower Cretaceous Shinekhudag Formation is about 250 m thick and composed of alternating beds of shale and dolomite. The Middle Jurassic Eedemt Formation is about 150 m thick and composed of alternating beds of shale, dolomitic marl, and siltstone. The alternations of shale and dolomite in both formations were formed by lake level changes, reflecting precipitation changes. Shales were deposited in the center of a deep lake during highstand, while dolomites were formed by primary precipitation during lowstand. Based on the radiometric age dating, the Shinekhudag Formation was deposited between (123.8 ±2.0) Ma and (118.5 ±0.9) Ma of the early Aptian. The Eedemt Formation was deposited at around 165–158 Ma of Callovian–Oxfordian. The calculated sedimentation rate of the Shinekhudag Formation is between (4.7 ±2.6) cm/ky and (10.0 ±7.6) cm/ky. Shales in the Shinekhudag Formation show micrometer-scale lamination, consisting of algal organic matter and detrital clay mineral couplets. Given the average thickness of micro-laminae and calculated sedimentation rate, the micro-lamination is most likely of varve origin. Both Middle–Upper Jurassic and Lower Cretaceous lacustrine oil shales were deposited in intracontinental basins in the paleo-Asian continent. Tectonic processes and basin evolution basically controlled the deposition of these oil shales. In addition, enhanced precipitation under humid climate during the early Aptian and the Callovian–Oxfordian was another key factor inducing the widespread oil shale deposition in Mongolia.

KEYWORDS

Cretaceous, humid climate, Jurassic, lake, Mongolia, oil shale, U–Pb age, varve

Toiruu34, Sukhbaatar, Ulaanbaatar 210646, Mongolia

[13]Department of Natural History Science, Hokkaido University, Kita 8, Nishi 5, Kita-ku, Sapporo 060-0810, Japan

[14]Graduate School of Environmental Studies, Nagoya University, Furo-cho, Chikusa-ku, Nagoya 464-8601, Japan

Correspondence
Hitoshi Hasegawa, Faculty of Science and Technology, Kochi University, Akebono-cho 2-5-1, Kochi 780-8520, Japan.
Email: hito_hase@kochi-u.ac.jp

Funding information
Grant-in-Aid for Scientific Research (B), Grant/Award number: 21403008 and 25302011; Fujiwara Natural History Foundation; Grant for Environmental Research Projects from the Sumitomo Foundation, Grant/Award number: 143485; Young Scientific Research (B), Grant/Award number: 25870309

1 | INTRODUCTION

Jurassic–Cretaceous sedimentary basins are widely distributed in the southern and eastern parts of Mongolia (Graham et al., 2001; Jerzykiewicz & Russell, 1991; Khand et al., 2000; Figure 1). Most of these basins are characterized by extensional tectonics of Late Jurassic to Early Cretaceous time formed by rifting and filled by syn-rift deposition. These well-developed rift basins in southeast Mongolia (e.g. Choibalsan, Tamsag, Choir-Nyalga, East Gobi and South Gobi basins; Figure 1) include lacustrine sedimentary succession containing thick oil shale and coal, which resemble the Daqing oil field of the Songliao basin of northeast China (Graham et al., 2001; Powell, 1986; Sladen & Traynor, 2000). Previous studies evaluated the potential of coal and petroleum resources in Jurassic–Cretaceous oil shale-bearing deposits in southeast Mongolia (Bat-Erdene, 2009; Bat-Erdene & Enkhtugs, 1987; Erdentsogt et al., 2009; Johnson et al., 2003; Johnson & Graham, 2004; Sladen & Traynor, 2000; Yamamoto et al., 1993, 1998). They are generally characterized by high content of total organic carbon (TOC), and thus the Lower Cretaceous organic-rich sediments are thought to be the petroleum source rocks (Johnson et al., 2003, Yamamoto et al., 1993, 1998). However, the age of the oil-prone lacustrine deposits in Mongolia is poorly constrained.

Recent paleontological study suggests that the oil-prone lacustrine deposits in Mongolia are not only of Early Cretaceous age, but also of the late Middle Jurassic (Li et al., 2014). Some studies also suggest that the Lower to Middle Jurassic sedimentary succession containing organic-rich lacustrine shales and coals has generated a significant hydrocarbon charge in Mongolia (Johnson et al., 2003, Sladen & Traynor, 2000). These lines of evidence indicate that potential oil-prone source rocks in Mongolia are not restricted to the Lower Cretaceous lacustrine strata but also included in Early–Middle Jurassic lacustrine strata, similar to the adjacent Chinese Jurassic basins (e.g. Tarim, Junggar and Ordos basins; Powell, 1986; Watson et al., 1987).

In this paper, we first review the general tectonic and stratigraphic framework of the Jurassic and Cretaceous lacustrine deposits in Mongolia. We then describe the lithostratigraphy and sedimentological characteristics of the type locality of both Jurassic and Cretaceous lacustrine oil shale deposits. We also provide new radiometric

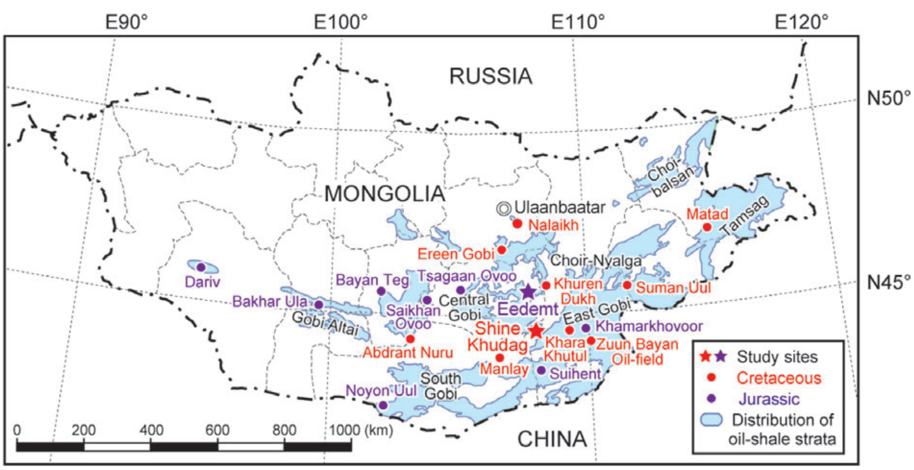

FIGURE 1 Map illustrating the distribution of Jurassic–Cretaceous lacustrine oil shales in Mongolia. Key localities for Cretaceous (red) and Jurassic (purple) sites are shown. Modified after Bat-Erdene (2009)

age data of intercalated tuff and basalt in order to establish detailed depositional ages for the Jurassic and Cretaceous lacustrine oil shale deposits in Mongolia. Based on the U–Pb and fission track (FT) ages of zircons in tuff layers, and on the K–Ar age of the basalt, late Middle–early Late Jurassic and late Early Cretaceous ages of the Mongolian lacustrine oil shales is presented.

2 | TECTONIC SETTING OF JURASSIC–CRETACEOUS BASINS IN MONGOLIA

Mongolia is situated in the heart of the Central Asian Orogenic Belt, which is fringed by the Siberian Craton in the north, essentially an amalgamation of lower Paleozoic terranes, and by the Northern China and Tarim Blocks in the south, an area of complex middle Paleozoic–Cenozoic terranes and suture zones (e.g. Badarch, Cunningham, & Windley, 2002; Lamb et al., 2008). By the Late Permian a major fold belt had been formed by the collision of the North China and Central Mongolian plates. The Upper Permian sedimentary strata include alluvial and fluvial deposits which incorporated thick bituminous coals and lacustrine shales. Thereafter, throughout the Mesozoic and Cenozoic, sedimentary deposits are distinctly non-marine, except for the Lower Triassic marine deposits of the northeastern margin of Mongolia (Ehiro, Zakharov, & Minjin, 2006). Based on the occurrence of the Lower Triassic *Lystrosaurus hedini* near the southern border of Mongolia (Noyon Uul area) and a lystrosaurid in the Lower Triassic of the Ordos basin in northern China, southern Mongolia likely had been connected to northern China as early as in the Early Triassic (Gubin & Sinitza, 1993; Hendrix et al., 1996).

One of the largest tectonic events affecting Mongolia and adjacent regions during the Mesozoic is attributed to the closure of the Mongol-Okhotsk Ocean from central Mongolia to the Okhotsk Sea with a scissor-like motion toward the northeast (Cogne et al., 2005; Donskaya et al., 2013; Metelkin et al., 2010; Yang et al., 2015; Zorin, 1999). Although the precise closure age of the Mongol-Okhotsk Ocean remains controversial, the closure of the ocean in the northeastern Mongolia region is thought to have occurred during the Middle–Late Jurassic. Yang et al. (2015) suggested that development of back-arc extensional basins with northeast–southwest orientation in southeast Mongolia and northeast China during the early Late Jurassic, prior to the final closure of the Mongol-Okhotsk Ocean. Such Middle–Upper Jurassic back-arc extensional basins then experienced strong compression, inversion and erosion during the latest Jurassic–earliest Cretaceous period (Graham et al., 2001; Meng, 2003; Yang et al., 2015). The timing of the compressional tectonics in south and southeast Mongolia is considered as late Late Jurassic (Kimmeridgian–Tithonian), which is constrained by radiometric dating of intercalated tuffaceous sandstone in the Sharilyn Formation

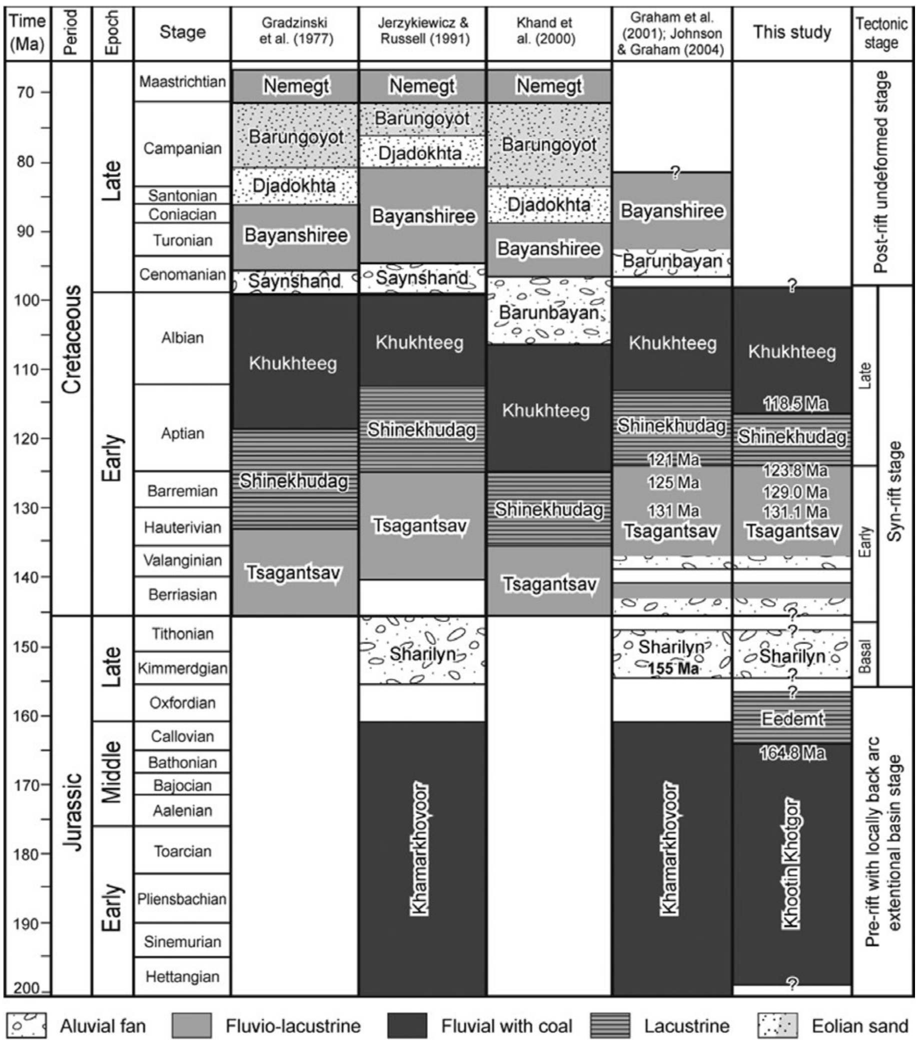

FIGURE 2 Comparison of chronostratigraphic subdivisions of Mongolian Jurassic–Cretaceous sedimentary successions and their inferred tectonic stages. Age assigned formations in each study are shown. Blank parts represent hiatus and/or formations with unknown ages

(155 Ma) in the Eastern Gobi basin (Graham et al., 2001: Figure 2). After the final closure of the Mongol-Okhotsk Ocean, numerous extensional basins with northeast–southwest orientation were developed in southeast Mongolia and northeast China during the Early Cretaceous.

Lower Cretaceous extensional sedimentary basins are widely developed in southeast Mongolia and northern China (Graham et al., 2001; Meng et al., 2003). Sedimentary successions of the basins display several depositional cycles, starting with alluvial and fluvial conglomerates and then passing upward into lacustrine fine-gained sedimentary rocks. Strike-slip faulting during rifting and/or inversion also occurred, as indicated by the occurrence of flower structures recorded on reflection seismic data (Graham et al., 2001; Johnson 2004). The basins were inverted at the end of the Early Cretaceous, and then overlain by relatively thin Upper Cretaceous sedimentary rocks (Graham et al., 2001; Meng et al., 2003).

3 | GENERAL STRATIGRAPHY OF JURASSIC–CRETACEOUS FORMATIONS IN MONGOLIA

Jurassic–Cretaceous sedimentary successions in Mongolia are characterized by three stages of tectonic regime; (i) pre-rift stage (Khamarkhovoor Formation) of the Early–Middle Jurassic age; (ii) syn-rift extensional stage of the Upper Jurassic to Lower Cretaceous succession (Sharilyn, Tsagantsav, Shinekhudag, Khukhteeg Formations); and (iii) mid-Cretaceous inversion and Upper Cretaceous post-rift succession (Barunbayan, Bayanshiree, Djadokhta, Barungoyot, Nemegt Formations) (Graham et al., 2001; Hendrix et al., 1996; Johnson & Graham, 2004; Traynor & Sladen, 1995; Figure 2).

The Lower–Middle Jurassic Khamarkhovoor Formation, exposed in the East Gobi, South Gobi, Gobi Altai, Mongol Altai, Khangai, and Lang Shan (Inner Mongolia) areas, consists of acidic–intermediate volcanics and coarse-grained sediments formed in alluvial fan environments with bituminous coals and floodplain lacustrine mudstones (Jerzykiewicz & Russell, 1991; Sladen & Traynor, 2000). Due to the compressional tectonics, the Early–Middle Jurassic was generally a time of widespread erosion resulting in the limited distribution of the Khamarkhovoor Formation. At the type section (Khamarkhovoor area), the formation is well exposed along the margins of basement uplifts of the Unegt subbasin in East Gobi, which is interpreted to be coeval with sedimentary deposits exposed at the Noyon Uul locality of South Gobi (Graham et al., 2001; Hendrix et al., 1996) and at the Dariv locality of southwestern Mongolia (Graham et al., 1997) (Figure 1).

The initiation of the syn-rift stage is marked by a distinctive approximately 250 m thick alluvial to fluvial conglomerate (Upper Jurassic Sharilyn Formation). The Sharilyn Formation consists of reddish colored breccias, conglomerates and fining-upward succession composed of red and green mudstone with some calcrete horizons (Graham et al., 2001). The Sharilyn Formation is assigned to the Late Jurassic (Kimmeridgian–Tithonian) based on freshwater assemblages such as molluscs, ostracodes and charophytes (Jerzykiewicz & Russell, 1991; Keller & Hendrix, 1997; Shuvalov, 2000), and by $^{40}Ar/^{39}Ar$ age of 155 Ma from a tuffaceous sandstone sample (Graham et al., 2001).

The overlying Lower Cretaceous succession is composed of alluvial fan to fluvio-lacustrine deposits of the Tsagantsav Formation, lacustrine deposits of the Shinekhudag Formation, and coal-bearing fluvial deposits of the Khukhteeg Formation, in ascending order. The Tsagantsav Formation reaches up to 1 km in thickness and the sediments are regarded as the main part of the syn-rift sequences by Graham et al. (2001). The formation consists mainly of fining upwards succession from the basal conglomerate to trough cross-bedded, coarse- to medium-grained sandstone, reddish or greenish shale, and calcretes. Although the overall climate during the period of the Tsagantsav Formation is thought to be dry due to the existence of reddish beds with calcretes, intermittently humid climate phases possibly existed during this period due to existence of some perennial lacustrine bodies. Graham et al. reported $^{40}Ar/^{39}Ar$ age of (131 $\pm$1) Ma (Khara Khutul section) and (126 $\pm$1) Ma (Tsagan Tsav section) of the intercalated basalts in the middle parts of the formation, suggesting a Hauterivian–Barremian age. Plant fossil evidence also indicates a Valanginian to Barremian age (Krassilov, 1982).

The Shinekhudag Formation is composed mainly of well-laminated shale (paper shale), dolomitic marls, dolomite, and siltstone, which represent characteristics of offshore lacustrine facies in large, perennial lakes. Detailed descriptions of this formation are provided in the next section. The Khukhteeg Formation, about 150–300 m thick, is composed mainly of dark greyish coaly mudstone, light greyish sandstones, and conglomerates. It is widespread in the east and center of Mongolia with the characteristic feature of abundant coal mine (e.g. Shivee Ovoo, Tevshin Gobi, Bayan Erkhet, Khuren Dukh, Nalaikh, Baga Nuur localities). Abundant partial tree trunks and other water-borne organic materials are intercalated in this formation (Shuvalov, 2000; Sochava, 1977). The Khukhteeg Formation also yields aquatic champsosaurs (Shuvalov, 2000) and trionychid turtles (Nessov, 1985; Vitek & Danilov, 2014). Spores and gymnosperm pollen are common in all areas, but pollens of ginkos are much less abundant (Ichinnorov 1998, 2005; Ichinnorov & Hofman, 2012). Angiosperms are also observed but are subordinate. The Khukhteeg Formation is dated as Albian or Aptian–Albian based on the basis of stratigraphic occurrences of molluscs, turtles and mammals (Shuvalov, 1975), and pollen-spores (Ichinnorov, 1998, 2005; Ichinnorov & Hofman, 2012; Nichols, Matsukawa, & Ito, 2006).

A period of structural inversion occurred during the mid-Cretaceous, which resulted in tilting and erosion of underlying syn-rift strata. These sediments are overlain by flat-lying Upper Cretaceous strata (Graham et al., 2001; Jerzykiewicz & Russell, 1991; Johnson, 2004; Figure 2). Flat-lying Upper Cretaceous strata of Mongolia, divided into the Barunbayan, Bayanshiree, Djadokhta, Barungoyot, and Nemegt Formations, in stratigraphically ascending order, are mostly reddish colored and preserve a near-continuous succession from the Cenomanian to Maastrichtian (Gradzinski, Kielan-Jaworowska, & Maryanska, 1977; Hasegawa et al., 2009; Jerzykiewicz & Russell, 1991; Khand et al., 2000; Martinson, 1982; Shuvalov, 2000; Sochava, 1975; Van Itterbeeck et al., 2005). The erosional unconformity between the Khukhteeg and Barunbayan Formations, which is not identified in outcrop but penetrated in drilled cores at Zuun Bayan oil field, is correlated to the lower boundary of the Upper Cretaceous succession in the South Gobi Basin (Graham et al., 2001). The upper contact of the Barunbayan Formation with the overlying Bayanshiree Formation is gradational (Martinson, 1982). Although the age of the Barunbayan Formation is controversial, similar assemblages of ostracods, molluscans, and charophytes occur from Albian to Cenomanian strata in eastern Asia (Barsbold, 1972; Makulbekov & Kurzanov, 1986). Thus, rift deformation and inversion are thought to be completed at around the transition from the Albian to the Cenomanian.

4 | LITHOSTRATIGRAPHY OF JURASSIC AND CRETACEOUS LACUSTRINE DEPOSITS

Since 2009, we have investigated the oil-prone lacustrine deposits in the Shine Khudag locality (type section of the Lower Cretaceous Shinekhudag Formation) in the Shaazangiin Gobi area, and the Eedemt locality in the Khootiin Khotgor area (Ando et al., 2011). The latter deposits, the Eedemt Formation in the Eedemt locality, is newly assigned to the late Middle Jurassic age on the basis of conchostracan assemblages (Li et al., 2014). In this section, we describe in detail the geology and lithostratigraphy of the Shinekhudag Formation in the Shine Khudag locality, and the Eedemt Formation in the Eedemt locality.

4.1 | Shine Khudag locality

The Shinekhudag Formation, well exposed in the type section of the Shine Khudag locality in the Shaazangiin Gobi area in the Dornogobi Province, is composed of alternating beds of dark grey paper shale (oil shale), light grey dolomitic marl, yellowish to brownish dolomite, and rare occurrence of silty mudstone layers (Figures 1, 3, and 4). Here, the Shinekhudag Formation is about 250 m thick and overlies the fluvio-lacustrine Tsagantsav Formation. It is overlain by the coal-bearing fluvial deposits of the Khukhteeg Formation. Strata mainly dip toward the north to northwest (dip angle: approximately 10°–20°), and they are cut by northwest–southeast directed strike-slip faults (Figure 3b). The middle to upper parts of the Shinekhudag Formation are well exposed in this area (N44°43′00″, E107°55′45″; Figures 3c and 4a–c). The alternations of shale, dolomitic marl and dolomite are rhythmically bedded in decimeter-, meter-, tens of meter-scale (mainly meter-scale; Figures 3c and 4b,c). The lowermost part of the formation is exposed along the banks of a dry creek (N44°42′45″, E107°55′15″), and composed mainly of light grey dolomitic marl and grey calcareous shales with minor amounts of dark grey shales (Figure 4d). Dark grey shale is well-laminated. Microscopic inspection reveals that laminae in shale is composed of micrometer-scale lamination, consisting of couplets of organic matter and detrital clay minerals (Figure 4g,h). Micritic texture of calcite crystals is also occasionally present just above the organic matter laminae (Figure 4h). In contrast, dolomitic marls and dolomites show a micritic texture with only weak lamination or even no lamination (Figure 4i). Scanning electron microscope (SEM) images show that dolomite layers consist mainly of aggregates of micrometer-scale crystals, exhibiting sub-rounded morphology (Figure 4j). Some dolomite beds show peloidal textures, but lack a distinct oncolitic texture. There are no clear signs of epigenesis, replacement or secondary infill of large dolomite crystals. Both, shale and dolomite layers occasionally contain abundant pyrite framboids, indicating microbial sulfate reduction within anoxic pore- or bottom-waters. Thin layers of tuff are partly intercalated, and analcime is common in the deposits, indicating alkaline and saline lake water environments with a certain volcanic input.

The overlying Khukhteeg Formation is exposed mainly in the Khukh Teeg hills, about 3 km northwest of the main section of the Shine Khudag locality (N44°44′30″, E107°53′18″; Figures 3a and 4f). Here, the Khukhteeg Formation is composed of greyish to dark brownish coaly mudstone, greyish sandstones and conglomerates. Abundant remains of woody trunks and stromatolites are also found. The underlying Tsagantsav Formation, exposed in the southeastern part of the area, is composed of trough cross-bedded, medium- to coarse-grained sandstones and conglomerates of fluvial channel origin. Dark grey paper shales and greyish dolomitic marls are also partly intercalated within the channel fill deposits in the upper part of the Tsagantsav Formation (Figure 3a).

In 2013 and 2014, two scientific research cores (CSH01, CSH02) were drilled in this area (Figure 3a,b). CSH01 core is 150 m long, and covers the lower to upper parts of the Shinekhudag Formation (Figure 4a). CSH02 core is 192 m long, and covers the middle part of the Shinekhudag Formation to the lower part of the Khukhteeg Formation beneath the top of the Khukh Teeg hills (Figure 4f). CSH01 and CSH02 cores are correlated to the outcrop succession on the basis of a marker bed represented by a remarkably thick dolomite layer (Figure 3c). The boundary between the Shinekhudag and Khukhteeg Formations is not well exposed in outcrop, but is well observed in the CSH02 core (Figure 3a). We set the boundary by the first appearance of coaly mudstone in the Khukhteeg Formation.

The Shinekhudag Formation contains abundant fossil remains, such as dense occurrence of conchostracans (Figure 4e), ostracods, plant remains, bivalves, and gastropods. Yuan & Chen (2005) examined ostracode and conchostracan assemblages in the Shine Khudag locality; and correlated the Shinekhudag Formation to the Jiufotang Formation (Early Aptian; Sha, 2007) of Liaoning Province, northeastern China, based on the occurrence of *Yanjiestheria gobiensis and Neodiestheria mongolensis.* Although some studies assigned the age of this formation to the Hauterivian–Barremian based on ostracode assemblages (e.g. Khand et al., 2000), floral and molluscan evidence supports an Aptian or Barremian–Aptian age (Jerzykiewicz & Russell, 1991; Krassilov, 1982). The $^{40}Ar/^{39}Ar$ age of intercalated basalts in the upper part of the underlying Tsagantsav Formation (*ca* 126 Ma; Graham et al., 2001) is also consistent with an Aptian age for the Shinekhudag Formation.

4.2 | Eedemt locality

The Eedemt Formation, exposed in the Khootiin Khotogor area in Dundgobi Province is composed of brownish-grey paper shale (oil shale), light grey dolomitic marl, greyish siltstone, and a small amount of pebbly sandstone (Figures 1, 5, and 6a–c). Here, the Eedemt Formation is about 150 m thick, and overlies the coal-bearing fluvial deposits of the Khootiin Khotogor Formation (Figure 6d). The strata in the Eedemt locality mainly dip toward southeast (dip angle: ~15°).

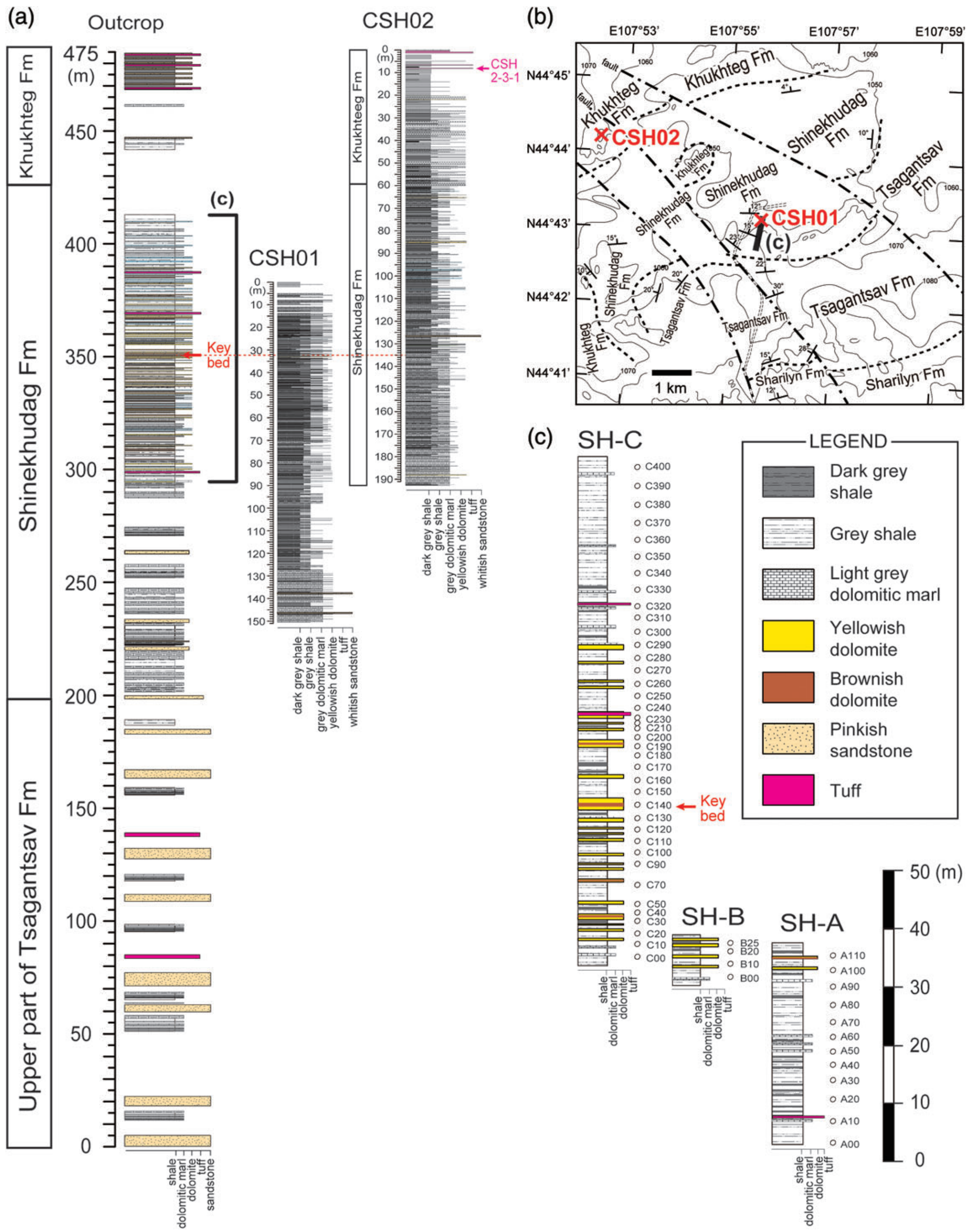

FIGURE 3 Geology (Lithostratigraphy) of the Shine Khudag locality. (a) Composite stratigraphic column of the Tsagantsav, Shinekhudag and Khukhteeg Formations at the Shine Khudag locality. Lithologic columns of two scientific research drill-cores (CSH01, CSH02) are also shown. Fm, Formation. (b) Geologic map of the Shine Khudag area. (c) Detailed stratigraphic columns of the middle to upper parts of the Shinekhudag Formation

The Eedemt Formation is well exposed in two sections named Eedemt A (ED-A: N45°41′10″, E107°43′20″) and Eedemt B (ED-B: N45°40′27″, E107°43′00″) (Figure 5a,b). We have also investigated a drill core (KH0818) (Figure 5c), which was drilled by the NEDO-MIT Joint Coal Expedition Project in 2008. The upper part of core KH0818 consists of the Eedemt Formation, while the basal part corresponds to the uppermost Khootiin Khotogor Formation. Although a clear lithological boundary between the Eedemt Formation and the underlying Khootiin Khotogor Formation is not exposed in outcrop, inspection of core KH0818 shows that the boundary is gradual.

The Eedemt Formation contains abundant fossil remains, such as conchostracans (Figure 6e), ostracods, plant remains, bivalves, and fish remains. Li et al. (2014) examined a conchostracan assemblage from the Eedemt locality, and described two new species, *Triglypta eedemtensis* Li sp. nov. and *Dundgobiestheria mandalgobiensis* Li gen. et sp. nov. Li et al. then demonstrated that *Triglypta* and *Dundgobiestheria* are common components of the Middle Jurassic *Euestheria ziliujingensis* and *Sinokontikia* faunas, and represents a typical taxon in the Middle Jurassic lacustrine sequences of northern Hebei, Junggar, and Turpan basins in northwest China. In

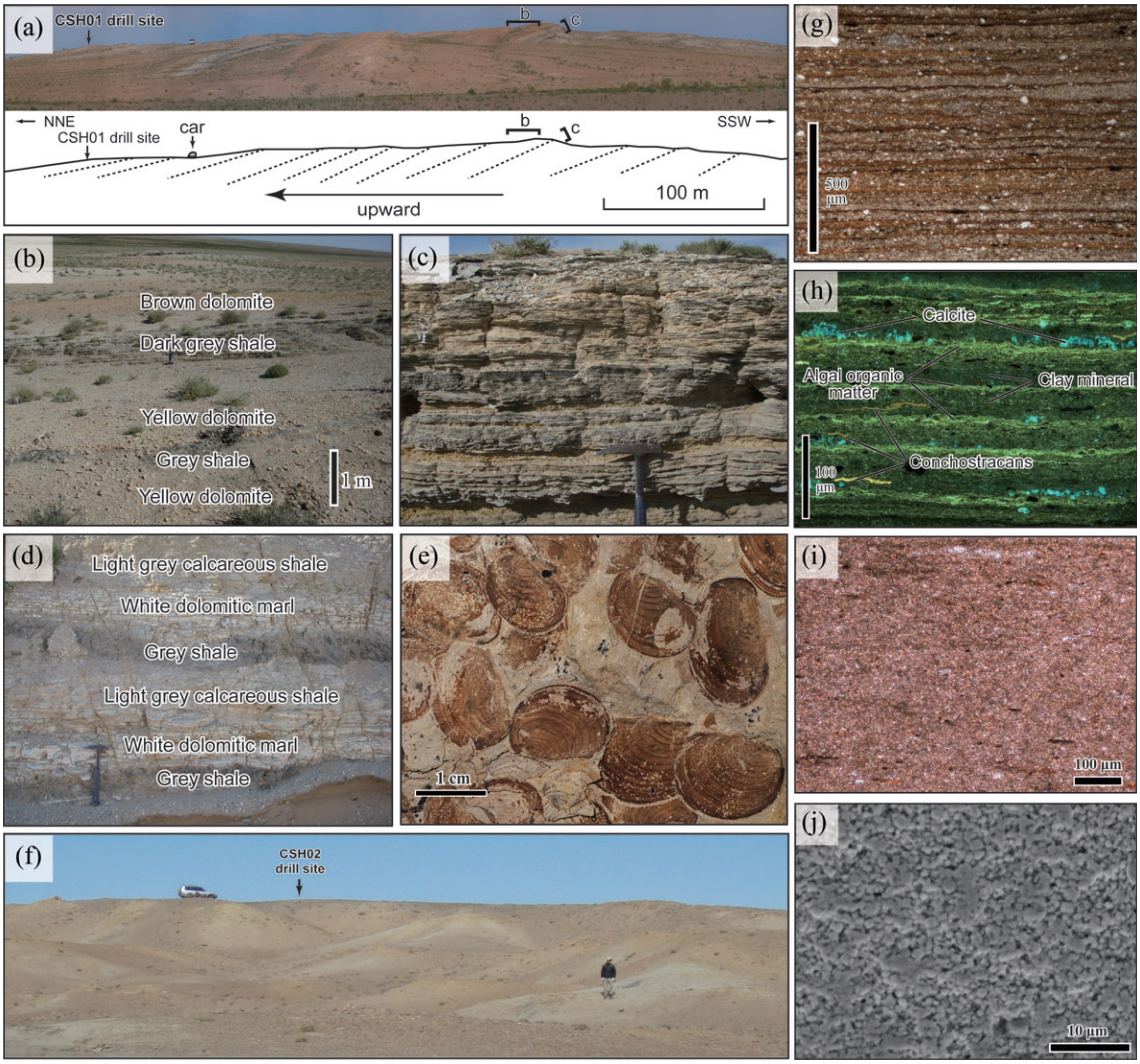

FIGURE 4 Outcrop photographs and photomicrograph of the Shinekudag Formation. (a) Overview of the Shine Khudag hill, which comprises the middle to upper parts of the Shinekhudag Formation. (b) Outcrop of meter-scale alternating beds of dark grey shale, grey shale, and yellowish to brownish dolomite (C10–C30 horizon of Figure 3b). (c) Outcrop of centimeter-scale alternating beds of dark grey shale and grey calcareous shale. (d) Outcrop photograph of meter-scale alternating beds of grey dolomitic marl, light grey calcareous shale, and grey shale along the banks of a dry creek, lowermost part of the Shinekhudag Formation. (e) Gregarious fossil occurrence of conchostracan (*Neodiestheria mongolensis*) on a bedding surface of the Shinekhudag Formation. (f) Overview of Khukh Teeg hill, the lower part of the Khukhteeg Formation in this area. (g) Photomicrograph of a dark grey paper shale layer showing micrometer-scale laminations. Dark brown coloured laminae is composed of algal organic matter, while light grey coloured laminae consists of detrital clay mineral. (h) Photomicrograph of reflected fluorescent image of micrometer-scale laminae in shale layer. Laminae couplets are mainly composed of highly fluorescent, light yellow-green coloured algal organic matter, and less fluorescent, dark-green coloured detrital clay mineral. Light blue coloured, calcite crystals of micritic texture commonly present just above algal organic matter laminae. Yellow coloured, cross section of conchostracans is also present within the clay mineral laminae. Average thickness of the laminae couplet in this photomicrograph is 60 μm. (i) Photomicrograph of a dolomite layer showing dense aggregates of micrometer-scale dolomite crystals. Weak lamination, consisting of brown coloured organic matter and dolomite crystals, are also observed. (j) Photomicrograph of scanning-electron micrometer (SEM) image of dolomite crystals showing dense aggregates of micrometer-scale crystals of sub-rounded morphology

particular, the *Dundgobiestheria* assemblage is correlated with the *Sinokontikia* fauna of the late Middle Jurassic (Callovian) age of the Qiketai Formation in the Turpan Basin, northwest China (Li et al., 2014). Therefore, the age of the Eedemt Formation is considered as late Middle Jurassic (Li et al., 2014). This interpretation is consistent with previous paleontological age constraints of the underlying coal-bearing strata of the Khootiin Khotgor Formation. Based on the floral evidence (Sodov, 1980, 1985, 1990) and recent palynological work by Ichinnorov, Purevsuren, and Buyantegsh (2008), the Khootiin Khotgor Formation is assigned to the Early–Middle Jurassic, and thought to be age equivalent to the Khamarkhovoor Formation (Figure 2).

5 | RADIOMETRIC AGE CONSTRAINTS

To establish the reliable chronology for the Shinekhudag and Eedemt Formations, U–Pb and FT age dating of intercalated tuff samples and K–Ar dating of intercalated basalt were conducted (Figures 7 and 8; Tables 1–3). U–Pb dating is applied to zircons from two tuff layers in

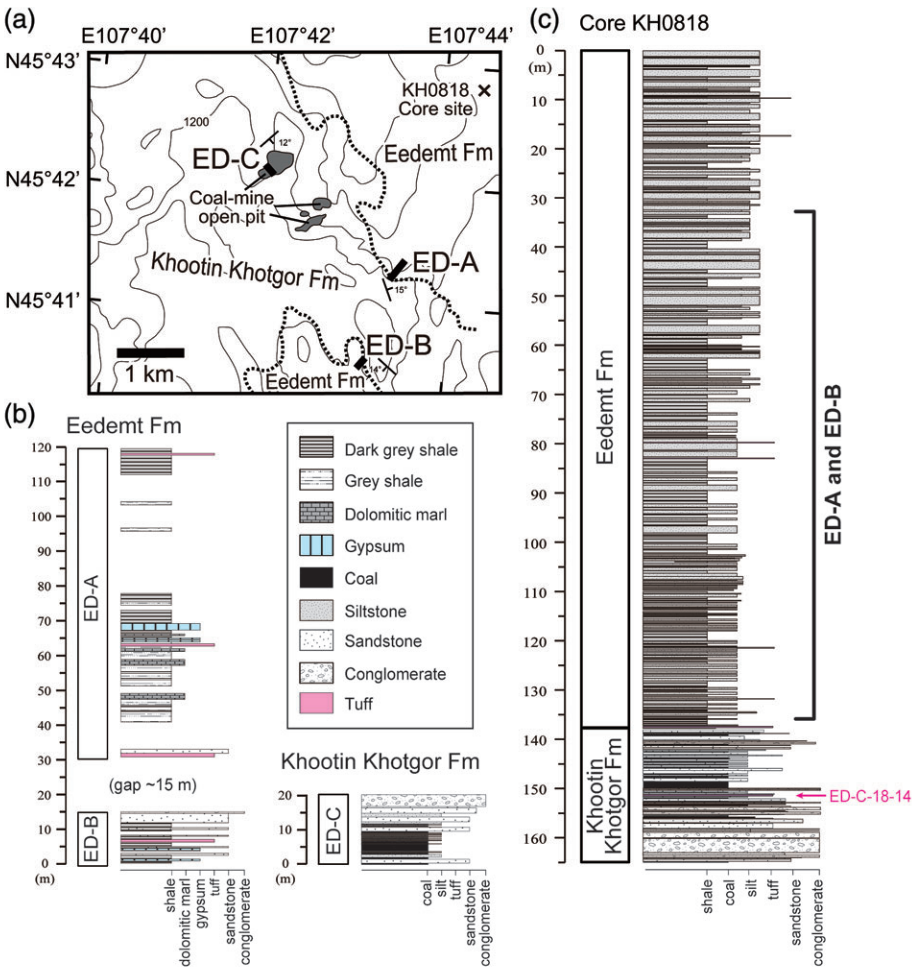

FIGURE 5 Geology (Lithostratigraphy) of the Eedemt locality. (a) Geologic map of Eedemt locality. (b) Stratigraphic column of main exposures of the Eedemt Formation (ED-A and ED-B) and the underlying Khootin Khotgor Formation (ED-C). (c) Lithologic column of drilled core (KH0818) showing the Eedemt Formation and the upper part of the Khootin Khotgor Formation. Correlated stratigraphic horizon of exposures of the ED-A and ED-B are shown

the lower part of the Khukhteeg Formation in the CSH02 core from the Shine Khudag area (sample CSH-2-3-1) and CMK-104 core from the Matad area, Dornod Province in eastern Mongolia (sample CMK-104-9), two tuff layers in the middle and upper parts of the Shinekhudag Formation in the CMK-104 and CMK-107 cores from the Matad area, (samples CMK-104-44 and CMK-107-50), a tuff layer in the uppermost part of the Tsagantsav Formation in the CMK-107 core from the Matad area (sample CMK-107-118), and from a tuff layer in the uppermost part of the Khootin Khotgor Formation in core KH0818 from the Eedemt area (sample ED-C-18-14) (Figures 3, 5, and 8). FT dating is also applied to zircons from a tuff layer in the uppermost part of the Khootin Khotgor Formation in core KH0818 from the Eedemt area (sample ED-C-18-14). K-Ar dating is applied to thick (150–200 m) basalt beds in the middle part of the Tsagantsav Formation from cores CMK-57 and CMK-58 drilled in the Suman Uul area, Sukhbaatar Province in eastern Mongolia (Figure 8).

5.1 | U–Pb and FT age

U–Pb dating of zircons from five tuff samples was conducted by Laser ablation–inductively coupled plasma–mass spectrometry (LA–ICP–MS) at Nagoya University. Numerous tuff and tuffaceous sandstone layers are intercalated in the lower part of the Khukhteeg Formation and the uppermost part of the Tsagantsav Formation in core samples derived from the Shine Khudag and Matad areas. Two samples (CSH-2-3-1, CMK-104-9) were taken from the lower part of the Khukhteeg Formation, two samples (CMK-104-44, CMK-107-50) were taken from the middle and upper parts of the Shinekhudag Formation, and one sample (CMK-107-118) was taken from the uppermost part of the Tsagantsav Formation (Figures 7a–e and 8; Table 1). One sample (ED-C-18-14) from the uppermost part of the Khootin Khotgor Formation was analyzed by both FT method and the U–Pb dating at Kanazawa University (Figure 7f; Tables 1 and 2). Zircons were extracted from tuff samples, and euhedral zircon crystals were mounted and polished. Extracted and polished zircons were first analyzed by using cathodeluminescence (CL) at Nagoya University to check potential differences in the internal structure.

The LA–ICP–MS analyses of extracted zircons were performed on an Agilent 7700× ICP–MS and Electro Scientific Industries NWR213 at Nagoya University. Zircon 91500 was used as an external standard for age calibration and the NIST SRM610 synthetic glass was applied for instrument optimization. In order to check the accuracy and reproducibility of the zircon ages, another zircon standard OD-3 (Iwano et al., 2013) was also analyzed. Several zircon crystals were measured from each sample and grains with negligible common lead (^{204}Pb is under the detection limit) were further considered. They were displayed in a concordia diagram (Figure 7) using Isoplot 3.75 (Ludwig, 2012), and grains plotted on the concordia within ±2 sigma error range were accepted to calculate weighted mean

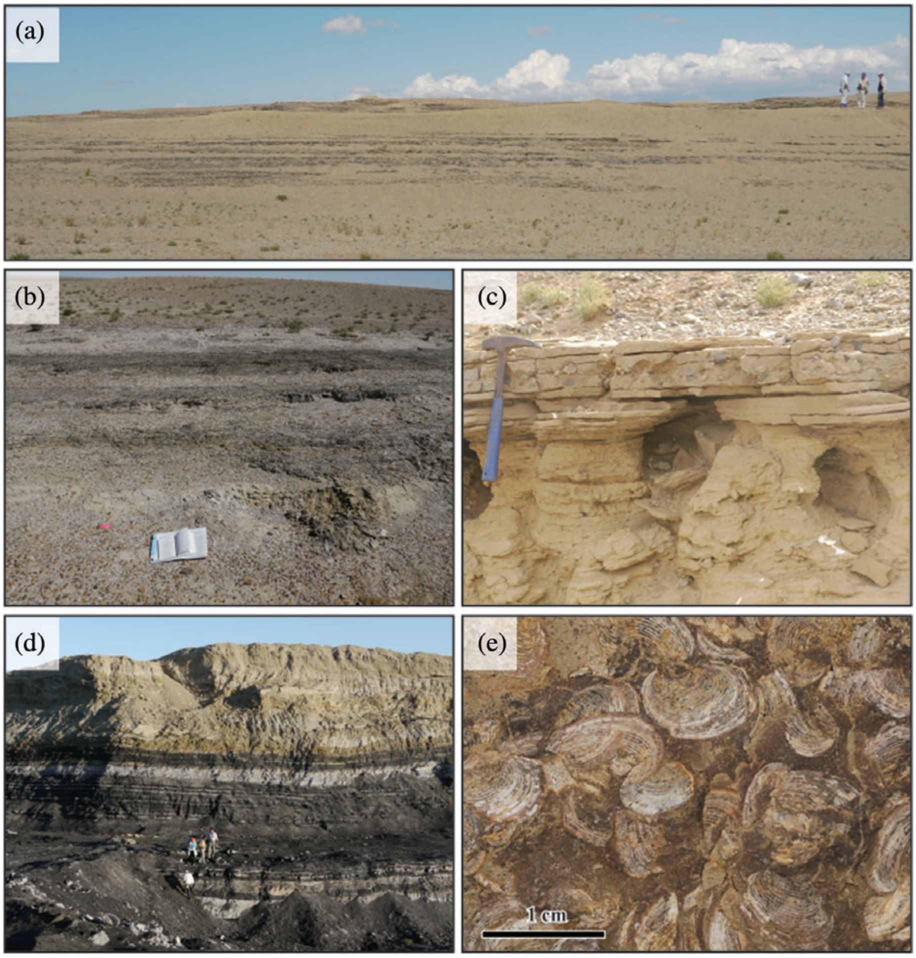

FIGURE 6 Outcrop photographs of the Eedemt Formation. (a) Overview of Eedemt hill (ED-A section), the lower part of the Eedemt Formation. (b) Outcrop of meter-scale alternating beds of brownish-grey paper shale, grey shale, and light greyish dolomitic marl in the ED-A section. (c) Outcrop of intercalated pebbly sandstone layer in the ED-B section. (d) Outcrop of coal seam, coaly mudstone, whitish sandstone of the upper part of the Khootin Khotgor Formation in the ED-C section at an open-pit coal mine. (e) Gregarious fossil occurrence of conchostracan (*Dundgobiestheria mandalgobiensis*) on a bedding surface of the Eedemt Formation

^{238}U–^{206}Pb and ^{235}U–^{207}Pb ages (Table 1). Because ^{238}U–^{206}Pb ages are more precise than ^{235}U–^{207}Pb ages, ^{238}U–^{206}Pb ages are accepted to discuss the depositional age of each formation. Experimental and instrumental details for U–Pb age dating at Nagoya University, and FT and U–Pb age dating at Kanazawa University are described in Kouchi et al. (2015) and Hasebe, Tamura, and Arai (2013), respectively, and references therein.

The U–Pb dating results (^{238}U–^{206}Pb ages) are shown in Figures 7 and 8. Two samples (CSH-2-3-1, CMK-104-9), taken from the lower part of the Khukhteeg Formation show the youngest ages of (118.5 ±0.9) Ma and (119.7 ±1.6) Ma. Two other samples (CMK-104-44, CMK-107-50) from the middle and upper parts of the Shinekhudag Formation show older ages of (121.0 ±0.9) Ma and (121.9 ±2.3) Ma. A single sample (CMK-107-118) taken from the uppermost Tsagantsav Formation shows the oldest age of (123.8 ±2.0) Ma. Thus, the depositional age of the Shinekhudag Formation can be constrained to range between (123.8 ±2.0) Ma and (118.5 ±0.9) Ma. The older age is consistent with the $^{40}Ar/^{39}Ar$ ages for tuff layers corresponding to the uppermost Tsagantsav Formation ((125 ±1) Ma) and the basal part of the Shinekhudag Formation ((121 ±1) Ma) as reported by Johnson and Graham (2004) (Figure 8). The FT and U–Pb ages of a tuff sample (ED-C-18-14) from the uppermost part of underlying Khootin Khotgor Formation analyzed at Kanazawa University are consistent within two sigma error range ((164.8 ±2.0) Ma and (158 ±7) Ma; Tables 1 and 2), assuming that zircons from the analyzed tuff layer were crystallized not immediately after the time of eruption.

5.2 | K–Ar isotopic age

K–Ar dating has been applied to two samples (CMK-57-72, CMK-58-17) taken from two basalt layers in the middle part of the Tsagantsav Formation in the Suman Uul area in eastern Mongolia (Figure 8). The basalt layers show baked basal contacts and weathered and vesicular tops. The basalts are generally fine grained, and include calcite veins. Thus, fresh samples lacking calcite veins were selected. K–Ar analysis and extraction of plagioclase from basalt samples were carried out at Hiruzen Institute for Geology & Chronology, Japan. Plagioclase crystals were extracted from crushed basalt samples by conventional mineral separation (50–75 μm). To remove alteration influences, extracted plagioclase samples were treated with HCl solution. Detailed analytical procedures of K–Ar method in Hiruzen Institute for Geology & Chronology are described in Itaya et al., (1991). Resultant ages are (131.1 ±2.8) Ma for CMK-57-72 and (129.0 ±2.8) Ma for CMK-58-17 (Table 3; Error estimate is σ throughout). These values are consistent with the existing $^{40}Ar/^{39}Ar$ ages ((126 ±1) Ma and (131 ±1) Ma) reported by Graham et al. (2001) for corresponding basalt layers in the middle part of the Tsagantsav Formation.

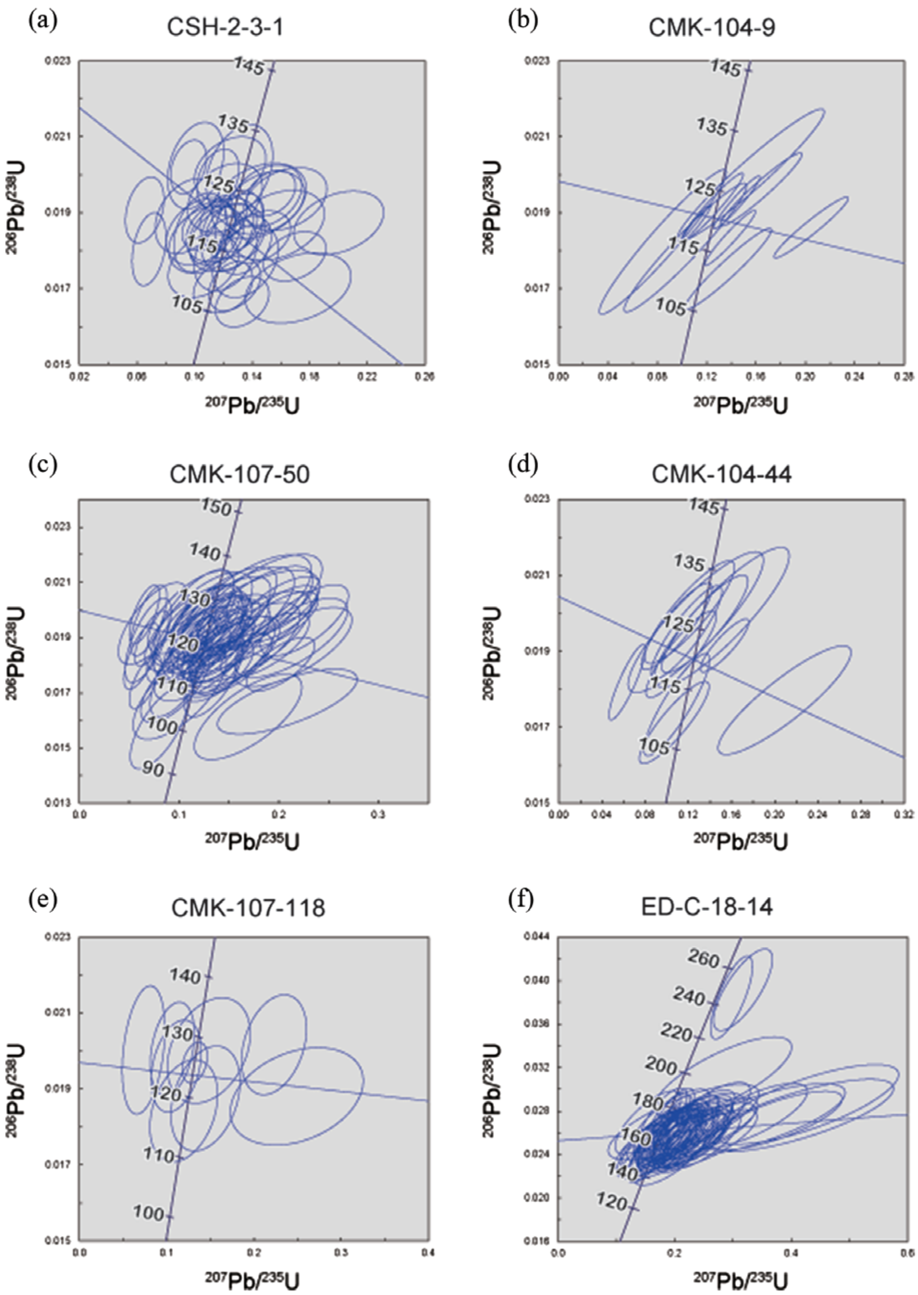

FIGURE 7 U–Pb concordia diagrams for tuff samples. (a,b) The lower part of Khukhteeg Formation in Shine Khudag and Matad sections. (c,d) The upper part of the Shinekhudag Formation in Matad section. (e) The uppermost Tsagantsav Formation in Matad section. (f) The basal part of the Eedemt Formation in Eedemt section

6 | DISCUSSION

6.1 | Age of the Shinekhudag and Eedemt Formations

Paleontological age constraints of the Shinekhudag Formation have been discussed controversially. Although abundant molluscan and ostracod fossils have been cited as evidence of a Barremian–Hauterivian age (Khand et al., 2000; Martinson & Shuvalov, 1973), an Aptian age of the formation was suggested by floral, conchostracans, and palynological evidence (Graham et al., 2001; Ichinnorov 1998, 2005; Ichinnorov & Hofman, 2012; Jerzykiewicz & Russell, 1991; Krassilov, 1982; Yuan & Chen, 2005). Martinson and Shuvalov (1973) previously considered a Hauterivian–Barremian age for the formation based on a conchostracans assemblage containing *Bairdestheria sinensis* (Chi), *B. mattoxi* Krassilov, and *Pseudograpta asanoi* (Kobayashi et Kusumi) from the lacustrine shale of the lower part of the Zuunbayan Formation (correlative strata of the Shinekhudag Formation) of East Gobi. Some of the lacustrine shales within the Tsagantsav Formation possibly were mistakenly correlated to the Shinekhudag Formation, as pointed out by Graham et al. (2001). On the other hand, Krassilov (1982) defined the age of the Shinekhudag Formation as Aptian, on the basis of two floral assemblage zones including *Baierella hastata*–*Araucaria mongolica*, and *Limnothetis gobiensis*–*Limnoniobe insignis*, which also occur in dated strata in eastern Siberia. Based on the conchostracan assemblage from the Shine Khudag locality, Yuan and Chen (2005) concluded that the Shinekhudag Formation can be correlated to the Jiufotang Formation of the Liaoning Province, northeastern China, given its similar faunal composition, whose age was assigned to the Early Aptian (Sha, 2007). In addition, Ichinnorov (1998, 2005) and Ichinnorov and Hofman (2012) report pollen and spore assemblages from the Shinekhudag Formation from Bayan

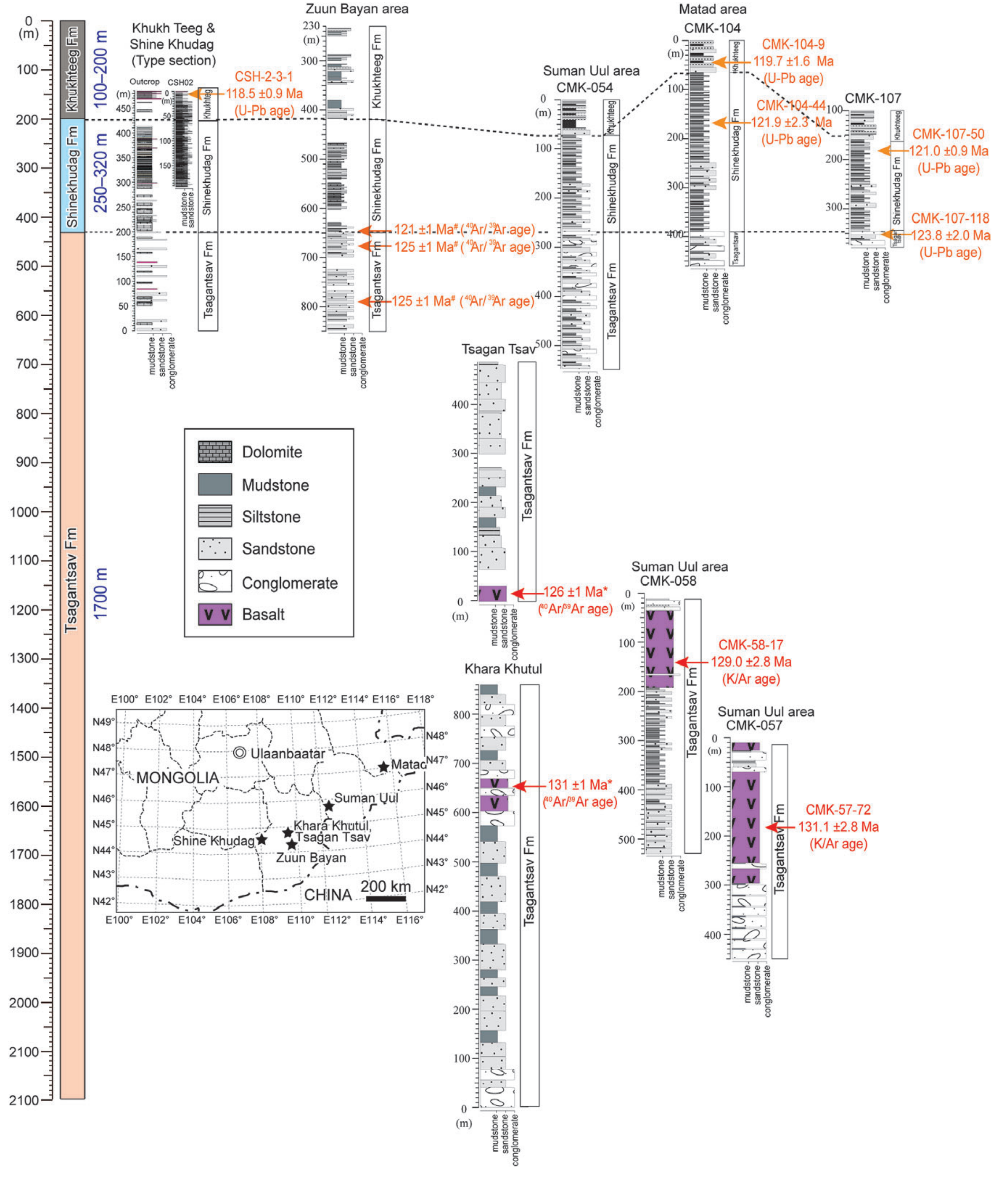

FIGURE 8 Litho- and chronostratigraphic correlation of the Tsagantsav, Shinekhudag, and Khukhteeg Formations in several sections in southern to eastern Mongolia. $^{40}Ar/^{39}Ar$ age* of intercalated basalt in Khara Khutul and Tsagan Tsav localities are from Graham et al. (2001). $^{40}Ar/^{39}Ar$ age# of intercalated tuffs in core sample of Zuun Bayan oil field are from Johnson and Graham (2004). K/Ar age of intercalated basalt in Matad locality, and U–Pb age of intercalated tuff in Shine Khudag and Matad localities are from this study. Fm, Formation

Erkhet, Matad, and Shine Khudag localities, which support an Aptian age for the formation.

On the basis of our U–Pb age dating of zircons in intercalated tuff samples, the Shinekhudag Formation is considered to be deposited between (123.8 ±2.0) Ma and (118.5 ±0.9) Ma of the Early Aptian (Figures 7 and 8). $^{40}Ar/^{39}Ar$ age data of intercalated tuff samples from a drillcore of the Zuun Bayan oil field (Johnson & Graham, 2004), which yielded (121 ±1) Ma in the basal part of the

TABLE 1 Zircon U–Pb dating results of the lower part of the Khukhteeg Formation, the upper part of the Shinekhudag Formation, the uppermost Tsagantsav Formation in Shine Khudag and Matad sections, and the basal part of the Eedemt Formation in Eedemt section

Sample name	Number of grains for concordia diagram	Number of concordant grains	$^{206}U/^{238}U$ Average ratio	$^{206}U/^{238}U$ Standard deviation	$^{206}U/^{238}U$ Weighted mean age (Ma)	$^{206}U/^{238}U$ Error (2σ) (Ma)	$^{207}U/^{235}U$ Average ratio	$^{207}U/^{235}U$ Standard deviation	$^{207}U/^{235}U$ Weighted mean age (Ma)	$^{207}U/^{235}U$ Error (2σ) (Ma)
CSH-2-3-1	37	25	0.018 6	0.000 8	118.5	0.9	0.126	0.014	120.3	3.4
CMK-104-9	10	8	0.018 7	0.000 7	119.7	1.6	0.125	0.022	122.2	6.3
CMK-107-50	64	49	0.019 0	0.000 8	121.0	0.9	0.139	0.025	136.7	4.2
CMK-104-44	12	9	0.019 1	0.001 0	121.9	2.3	0.121	0.014	121.6	10.5
CMK-107-118	10	7	0.018 9	0.001 4	123.8	2.0	0.122	0.018	122.4	8.0
ED-C-18-14	64	48	0.024 7	0.001 1	164.8	2.0	0.201	0.026	184.2	5.7

TABLE 2 Zircon fission track (FT) dating result of the basal part of the Eedemt Formation in Eedemt section

FT dating sample name	Number of grains	Number of FT	FT density (10^6/cm^2)	LA–ICP–MS data: Zr Average $^{238}U/^{29}Si$	Zr Standard deviation (%)	NIST610 Average $^{238}U/^{29}Si$	NIST610 Standard deviation (%)	Pooled mean Zr/NIST610 ($^{238}U/^{29}Si$)	Error (2σ) (%)	Pooled mean U (mg/g)	Pooled mean age (Ma)	Error (2σ) (Ma)
ED-C-18-14	61	3 475	5.747	0.079 3	40	0.230	7	0.324	0.64	70.3	158	7

TABLE 3 Result of K–Ar dating of basalt samples in the middle part of the Tsagantsav Formation in Suman Uul section

Sample name	K content (wt%)	Average K (wt%)	Radiogenic ^{40}Ar (10^{-8} cc STP/g)	K–Ar age (Ma)	Atmospheric ^{40}Ar (%)
CMK-57-72	1.414	1.418 ±0.510	748.0 ±7.5	131.1 ±2.8	2.4
	1.422				
CMK-58-17	1.268	1.275 ±1.110	661.7 ±6.4	129.0 ±2.8	1.7
	1.282				

Decay constant: $\lambda_e = 0.581 \times 10^{-10}$/year, $\lambda_\beta = 4.962 \times 10^{-10}$/year, $^{40}K/K = 1.167 \times 10^{-4}$ (Steiger & Jager, 1977).

Shinekhudag Formation and (125 ±1) Ma age in the uppermost part of the underlying Tsagantsav Formation, and the K/Ar age ((129.0 ±2.8) Ma, (131.1 ±2.8) Ma; Table 3) and $^{40}Ar/^{39}Ar$ age ((126 ±1) Ma, (131 ±1) Ma; Graham et al., 2001) of the intercalated basalt in the upper Tsagantsav Formation are also consistent with our chronology for the Shinekhudag Formation (Figure 8). However, the error range of our U–Pb age and reported $^{40}Ar/^{39}Ar$ age of the boundary between the Shinekhudag Formation and the underlying Tsagantsav Formation overlap with each other. Thus, the precise age of the initiation of the Shinekhudag Formation needs further investigation. The total thickness of the Shinekhudag Formation is about 250 m in the type section of Shine Khudag and in most of the other sections (Figure 8). Given that the deposition of the Shinekhudag Formation was initiated at (123.8 ±2.0) Ma (our U–Pb age data) or (121 ±1) Ma ($^{40}Ar/^{39}Ar$ age of Johnson & Graham, 2004), and ended before (118.5 ±0.9) Ma (our U–Pb age data), the calculated sedimentation rate of the formation is in range between (4.7 ±2.6) cm/ky and (10.0 ±7.6) cm/ky.

Although the age of the lacustrine deposits in the Khootin Khotgor area (Eedemt Formation) was also controversial, Li et al. (2014) demonstrated the existed problems, and assigned its age as late Middle Jurassic. Li et al. demonstrated that the *Dundgobiestheria* assemblage is correlated with the *Sinokontikia* fauna of the late Middle Jurassic (Callovian) age of the Qiketai Formation in the Turpan Basin, northwest China. The age of the correlative strata in China (Tiaojishan Formation in northern Hebei basin) are also supported by radiometric age data (Li et al., 2014; Zhang, Wang, & Liu, 2008). Based on the U–Pb dating of intercalated tuff samples, the age of the Tiaojishan Formation is assigned as from 165 Ma to 156–153 Ma of late Middle–early Late Jurassic (Zhang et al., 2008).

On the basis of our U–Pb and FT age of a tuff sample (ED-C-18-14) in the uppermost part of the underlying Khootin Khotgor Formation, the Eedemt Formation is considered to be deposited at around 165–158 Ma of Callovian–Oxfordian (Figures 7 and 8; Gradstein et al., 2012). U–Pb and FT ages ((164.8 ±2.0) Ma and (158 ±7) Ma, respectively) are within two sigma error range, assuming that zircons from the analyzed tuff layer were crystallized not very early from the time of eruption. Given the age of the overlying Sharilyn Formation is assigned to the late Late Jurassic (Kimmeridgian–Tithonian) based on abundant freshwater assemblages such as molluscs, ostracodes and charophytes (Jerzykiewicz & Russell, 1991; Keller & Hendrix, 1997; Shuvalov, 2000), and $^{40}Ar/^{39}Ar$ age ((155 ±1) Ma; Graham et al., 2001) of the intercalated tuff in the middle Sharilyn Formation, the age of the Eedemt Formation likely includes Oxfordian. But the possibility of Callovian age is also not negligible due to the age constraints by conchostracans assemblages (Li et al., 2014). Conclusively, the age of the Eedemt Formation is considered to be deposited at around 165–158 Ma of Callovian–Oxfordian (late Middle–early Late Jurassic).

6.2 | Depositional environments of shale–dolomite couplets

Both, the Shinekhudag and Eedemt Formations are composed mainly of meter-scale alternating beds of dark grey shale, light grey dolomitic marl and dolomite, with minor amounts of siltstone and sandstone. Shale beds are generally well-laminated with no significant bioturbation (Figure 4g,h), indicating low-oxygen or anoxic bottom-water conditions. Permanent or at least seasonal stratification promotes the development of anoxic bottom waters in deep lakes with several tens of meters depth (O'Sullivan, 1983; Zolitschka et al., 2015). Tropical lakes in Africa (e.g. Lake Malawi and Lake Tanganyika) are examples of modern freshwater lakes where permanent stratification promotes stagnant anoxic bottom water and TOC-rich sediments (Brown, Callonnec, & German, 2000; Cohen et al., 2006). Palynological evidence for abundant green algae (incl. *Botryococcus*), and the presence of β-carotane in oil shale deposits of both formations indicate considerable algal export production in slightly saline to freshwater lakes with anoxic bottom waters (Johnson et al., 2003; Sladen & Traynor, 2000). Yamamoto et al. (1998) also reports geochemical evidence for blooming of autotrophic prokaryotes and thermal stratification with anoxic lake-bottom conditions in the East Gobi basin.

In contrast, dolomitic marl and dolomite beds show weakly laminated or no lamination, and are composed of aggregates of micrometer-scale sub-rounded dolomite crystals. Similar textures of the lacustrine dolomite with small, 1–2 μm crystal aggregates exhibiting sub-rounded morphology are reported from Pliocene deposits in Spain and Holocene deposits in France, which are interpreted to be formed by bacterially-induced dolomite precipitation in shallow saline lake environments (Breheret et al., 2008; Del Cura et al., 2001). Because of the lack of replacement textures, micro-crystalline dolomite is thought to represent autochthonous and primary precipitation from the lake water or early diagenetically from pore water. In addition, almost all modern lacustrine dolomite is formed primary within saline lake waters with a high Mg/Ca ratio, in association with biological activity (Last, 1991).

An observational study of modern lakes by Dean and Megard (1993) provides significant analogy for dolomite deposition and depositional environmental change of shale–dolomite couplets in the Shinekhudag Formation. The sediments of saline prairie lakes in western Minnesota, North Dakota, and South Dakota commonly contain high-Mg calcite and dolomite especially during the mid-Holocene dry climatic period. In contrast, low-Mg calcite is dominant in today's forest-dominant lake sediments under more humid climatic setting. Dean and Megard also demonstrated that changes in relative proportions of dissolved calcium and magnesium in lakes across the precipitation-evaporation gradient setting of 219 lakes from Wisconsin, North Dakota, and South Dakota (data from Gorham, Dean, & Sanger, 1982). In response to increasing salinity (decreasing lake-level) and precipitation of calcium carbonate, the relative proportion of calcium decreases and the relative proportion of magnesium increases. Hence, the precipitation of calcite results in an increase in the Mg/Ca ratio in lake water. Then, high Mg/Ca ratio in the arid saline lakes results in deposition of dolomite and high-Mg calcite in their sediments. Therefore, carbonate composition in lake sediments of the forest–prairie border setting should be a sensitive indicator of salinity variations in the lake, in response to climatically induced changes in the balance between precipitation and evaporation (Dean & Megard, 1993).

Given that the dolomite beds in the Shinekhudag Formation show no clear evidence of lacustrine littoral facies such as evaporative facies or desiccation structures (Johnson & Graham, 2004), the dolomite beds are likely to be formed by primary precipitation from the lake water in the lake center. Dry climatic periods would alter lake chemistry such that magnesium ions could be concentrated (e.g. Dean & Megard, 1993). Abundant green algae (e.g. *Botryococcus*) possibly have partly contributed magnesium ions as well. By analogy with prior studies of dolomite formation in lakes, the dolomite beds in the Shinekhudag and Eedemt Formations are likely to be formed by autochthonous and primary precipitation during phases of low lake level with possible influence of microbial mediation. Presence of calcite crystals within shale layers (Figure 4h) and predominance of dolomite crystals in dolomite layer are also consistent with the aforementioned observations by Dean and Megard (1993).

Conclusively, the meter-scale alternations of shale and dolomite were primarily controlled by lake level changes, which could have reflected changes in precipitation. Shale beds formed in the deep lake during lake level highstand of freshwater to slightly saline lake environment, while dolomite beds formed by autochthonous and primary precipitation during lowstand of saline lake environment with possible influence of microbial mediation. The common presence of analcime in tuff and shale layers is also consistent with alkaline and saline lake waters with a certain volcanic input (Remy & Ferrell, 1989).

6.3 | Origin of micrometer-scale lamination

As described above, shale beds in the Shinekhudag Formation include micrometer-scale laminations, which are composed of couplets of dark brownish colored organic matter-rich laminae and light greyish colored laminae composed of detrital clay minerals (Figure 4g). Reflected fluorescent microscopic inspection confirms that the dark brownish colored organic matter-rich laminae consist of highly fluorescent algal organic matter, while the light greyish colored laminae consist of less fluorescent detrital clay mineral (Figure 4h). Micritic texture of calcite crystals is also occasionally present just above the algal organic matter laminae (Figure 4h). These characters and orderings of the composition of lamina couplets are similar to the organic-clastic varve in lakes of temperate climatic setting as discussed below (e.g. Luder et al., 2006; Zolitschka et al., 2015).

In addition, the occurrence of calcite crystal above the organic-rich laminae is significantly consistent with observation of modern lake sediments by Dean and Megard (1993). Seasonal changes in primary productivity, carbonate saturation, water chemistry, and sediment-trap samples reveal that calcite precipitates during late summer, triggered by algal photosynthesis. The pH of the lake epilimnion increases to almost 9.0 in late summer in response to photosynthetic removal of CO_2 during the summer months (Dean & Megard, 1993). Thus, by analogy with existing studies of varve sediments in temperate lakes, algal organic matter laminae and micritic calcite crystals in shale layer of the Shinekhudag Formation are likely to be formed during the late spring to late summer, while detrital clay mineral laminae are dominant during autumn–winter.

Notably, our interpretation of the micrometer-scale laminations as annually-laminated varves can be strongly supported by the sedimentation rates. Given that the average thickness of the laminae couplets is about 50–70 μm in shale layers (Figure 4g,h) compared to about 100–120 μm thick, less pronounced lamination preserved in dolomitic marl facies (Figure 4i). If the laminae couplets in the Shinekhudag Formation are seasonal varves as discussed above, the average sedimentation rate is estimated to be approximately 50–120 μm/year, which corresponds to approximately 5–12 cm/ky. This estimate is consistent with the chronostratigraphically calculated sedimentation rate of (4.7 ±2.6) cm/ky to (10.0 ±7.6) cm/ky described above.

Varve couplets consisting of algal organic matter and detrital clay minerals in shale layers of the Shinekhudag Formation resemble a typical feature of modern and Quaternary lake sediments in the tropics and temperate latitudes, and they are categorized as organic-clastic varves (e.g. Brauer et al., 1999; Brown et al., 2000; Cohen et al., 2006; Enters et al., 2010; Luder et al., 2006; Ojala et al., 2012; Shanahan et al., 2008; Zolitschka et al., 2015). The dark brown colored organic-rich laminae were probably formed by phytoplankton remains produced as a result of late spring to summer blooms, while the light grey colored detritus clay-rich laminae represent allochthonous terrestrial input deposited during the autumn–winter season (Figure 4g). Since sedimentary grading structures are absent in the detrital laminae, formation of clay-rich laminae during rainy summer seasons is unlikely. Micritic calcite is occasionally preserved in just above the organic-rich part of individual laminae (Figure 4h), which possibly indicate formation via biochemically-induced precipitation during late summer season (Dean & Megard, 1993). This type of varve couplet composition indicates increased lake surface temperature and primary production during summer season as reported from modern mid-latitude lakes (e.g. Sacrower See Lake in Germany; Enters et al., 2010; Luder et al., 2006). Given that the lacustrine oil shales of the Shinekhudag Formation are also deposited in the mid-latitude, the distinct varve composition of this formation suggests existence of seasonality during the mid-Cretaceous "greenhouse" climate.

Shales in the Eedemt Formation also exhibit micrometer-scale lamination, suggesting the possibility of seasonal varve origin. However, the lack of precise absolute age control of the Eedemt Formation does not allow for reliable estimates of sedimentation rates. Further studies are needed to verify the origin of the micrometer-scale lamination pattern characterizing the Eedemt Formation.

6.4 | Tectonic-climatic setting of the Jurassic–Cretaceous lacustrine deposits

The paleo-latitudinal position of the Jurassic–Cretaceous sedimentary basins in Mongolia represents an important aspect for understanding potential trigger mechanisms for the widespread deposition of lacustrine oil shales at that time. The configuration of the paleo-Asian continent and the closure of Mongol-Okhotsk Ocean have been reconstructed based on paleomagnetic studies (Chen et al., 1993; Cogne et al., 2005; Halim et al., 1998; Hankard, Cogne, & Kravchinsky, 2005; Kravchinsky et al., 2002; Metelkin et al., 2010; Pruner, 1992; Yang et al., 2015; Zhao et al., 1990; Zorin, 1999). Based on the reconstructed paleogeographic map of the paleo-Asian continent, the Gobi basin was located at approximately 41°–44°N (Pruner, 1992) or approximately 45°–50°N (Cogne et al., 2005) during Early Cretaceous times, whereas it was located at 42°–55°N during the Middle–Late Jurassic (Cogne et al., 2005; Kravchinsky et al., 2002). Despite considerable uncertainties regarding the exact paleo-latitudinal position of the Gobi basin during the Middle Jurassic, a mid-latitudinal position at 40°–50° can be inferred for both the Middle–Late Jurassic and Early Cretaceous times.

Due to the different paleogeographic settings caused by the closure of the Mongol-Okhotsk Ocean (Kravchinsky et al., 2002; Metelkin et al., 2010; Yang et al., 2015), distance of the Gobi basin from coastline could be largely different between the Middle–Late Jurassic and the Early Cretaceous. In addition, the tectonic settings of the Jurassic and Cretaceous sedimentary basins are also different. Nevertheless, both of the lacustrine oil shales were thought to be deposited in intracontinental extensional basins in mid-latitudes of paleo-Asian continent during the late Middle–early Late Jurassic and the late Early Cretaceous. Early Cretaceous extension was possibly resulted from strike-slip faults that bounded the plate fragments in China and Mongolia. Although cause of the Middle–Late Jurassic extension is currently unclear, combination of causes was possibly responsible for extensional basin development, i.e. both subduction-related and strike-slip-related extension led to conditions ideal for lake basins (Sladen & Traynor, 2000). Tectonic processes and basin evolution basically controlled the deposition of these lacustrine oil shales. In addition, the common occurrence of stratigraphically continuous lacustrine deep water deposits associated with coal-bearing fluvial strata in both, the Middle–Late Jurassic and the late Early Cretaceous indicate enhanced precipitation within a humid climatic setting during the early Aptian and the Callovian–Oxfordian times is more likely to be a key factor of the widespread occurrence of lacustrine environments in southeast Mongolia (e.g. Hasegawa et al., 2012).

It is noteworthy that the deposition of lacustrine oil shales in the Shinekhudag Formation occurred between (123.8 ±2.0) Ma and (118.5 ±0.9) Ma of early Aptian, which is nearly contemporary to the one of the largest Ocean Anoxic Events (OAE) of OAE1a interval (Emeis & Weissert, 2009; Erba et al., 2015; Follmi, 2012). In addition, the depositional interval of the Eedemt Formation at around Callovian–Oxfordian is also nearly accordant to the recently recognized OAE event during the Callovian–Oxfordian (e.g. Hautevelle et al., 2007; Louis-Schmid et al., 2007; Nozaki, Kato, & Suzuki, 2013; Rais et al., 2007; Weissert, 2011).

7 | SUMMARY

The present study explored the spatial and temporal distribution of the Mongolian oil shales, and established detailed ages for the Jurassic and Cretaceous lacustrine deposits in Mongolia. The Lower Cretaceous Shinekhudag Formation, which is widely distributed in southeastern Mongolia, is composed of meter-scale alternating beds of shale and dolomite. At the type locality of the Shine Khudag area, the formation is about 250 m thick and overlies the fluvio-lacustrine Tsagantsav Formation, and is overlain by the coal-bearing fluvial deposits of the Khukhteeg Formation. The Middle–Late Jurassic Eedemt Formation is composed of alternations of shale, dolomitic marl, silt- and sandstone. In the type locality of the Khootin Khotogor area, the formation is 150 m thick, and overlies the coal-bearing fluvial deposits of the Khootin Khotogor Formation. Meter-scale alternating beds of shale and dolomite are thought to record fluctuations in lake level, which was primarily controlled by precipitation changes. Namely, shale beds were deposited in the center of a deep lake during a highstand phase of freshwater to slightly saline environment, while dolomite beds were formed by autochthonous and primary precipitation during lowstand phase of saline lake environment with possible influence of microbial mediation.

To establish a detailed chronology of these lacustrine deposits, FT and U–Pb age dating of zircons derived from intercalated tuffs and K–Ar age dating of intercalated basalts were carried out. Based on the new radiometric age dating, the Shinekhudag Formation was deposited between (123.8 ±2.0) Ma and (118.5 ±0.9) Ma of early Aptian times, while the Eedemt Formation was deposited at around 165–158 Ma in the Callovian–Oxfordian, although precise ages of the both formations need further investigation. The calculated sedimentation rate of the Shinekhudag Formation is between (4.7 ±2.6) cm/ky and (10.0 ±7.6) cm/ky. Shales in the Shinekhudag Formation exhibit micrometer-scale laminations, which are composed of couplets of algal organic matter and detrital clay minerals. Given an average thickness of the micro-lamination of about 50–70 μm in shale facies compared to about 100–120 μm in dolomitic marl facies, the micro-laminations in the Shinekhudag Formation are most likely of varve origin reflecting seasonal cyclicity.

Lacustrine oil shales of both the Middle–Late Jurassic and the late Early Cretaceous ages were deposited in intracontinental extensional basins in the mid-latitudes of the paleo-Asian continent. Although basin tectonics may have affected the deposition of these lacustrine oil shales, enhanced precipitation within a humid climatic setting during the early Aptian and the Callovian–Oxfordian times is more likely to be a key factor of the widespread occurrence of lacustrine environments in southeast Mongolia. The depositions of the lacustrine oil shales, both in the Shinekhudag Formation at around 123–119 Ma and in the Eedemt Formation at around Callovian–Oxfordian, are nearly contemporary to reported OAE intervals.

ACKNOWLEDGEMENT

We are grateful to B. Gantsolmon, S. Kito, S. Yogo, M. Nozaki and A. Matsumoto for their analytical and technical assistance. We are also grateful to Enkhtogs and Orgil of Cameco Mongolia LLC for donation of chronological samples. We also appreciate to Y. Kouchi for comments and corrections for the U–Pb age data. We are also grateful to R. Barsbold, K. Tsogtbaatar, Y. Khand, N. Katsuta and F. Hirsch for fruitful comments of the manuscript. We are also grateful to detail and constructive reviews by Y. I. Lee, H. Weissert, and AE S. Bajpai. This paper is a contribution to UNESCO-IUGS IGCP608 "Cretaceous ecosystems and their responses to paleoenvironmental changes in Asia and the Western Pacific". This study was supported financially by Grant-in-Aid for Young Scientific Research (B) (No. 25870309), Grant for Environmental Research Projects from the Sumitomo Foundation (143485), and Fujiwara Natural History Foundation provided to H. Hasegawa, and Grant-in-Aid for Scientific Research (B) (No. 21403008 and 25302011) provided to H. Ando.

ORCID

Hitoshi Hasegawa http://orcid.org/0000-0003-0925-2717

REFERENCES

Ando, H., Hasegawa, H., Hasegawa, T., Ohta, T., Yamamoto, M., Hasebe, N., … Ichinnorov, N. (2011). Jurassic–Cretaceous lacustrine deposits in the East Gobi Basin, southeast Mongolia. *Journal of Geological Society of Japan*, *117*, XI–XII.

Badarch, G., Cunningham, D., & Windley, B. F. (2002). A new terrane subdivision for Mongolia: Implications fort the Phanerozoic crustal growth of Central Asia. *Journal of Asian Earth Sciences*, *21*, 87–100.

Barsbold, R. (1972). Biostratigraphy and fresh-water Molluscus from the Upper Cretaceous of Mongolia. Moscow, Russia: Izdatielstvo Nauka (in Russian).

Bat-Erdene, D. (2009). Mongolian oil shale basins and deposits. In J. Byamba (Ed.), *Fossil fuel. Mongolian geology and mineral resources* (Vol. *5*, pp. 178–271). Memorial Volumes to 70th Year Anniversary for Mongolian Geological Survey. Ulaanbaatar: Mongolian Geological Survey (in Mongolian).

Bat-Erdene, D., & Enkhtugs, O. (1987). Distribution and formation of coal deposits and coal-bearing basins. Ulaanbaatar, Mongolia: Geology and Exploration of Mongolian People's Republic (in Russian).

Brauer, A., Endres, C., Guenter, C., Litt, T., Stecich, M., & Negendank, J. F. W. (1999). High resolution sediment and vegetation responses to Younger Dryas climate change in varved lake sediments from Meerfelder Maar, Germany. *Quaternary Science Reviews*, *18*, 321–329.

Breheret, J. G., Fourmont, A., Macaire, J. J., & Negrel, P. (2008). Microbially mediated carbonates in the Holocene deposits from Sarlieve, a small ancient lake of the French Massif Central, testify to the evolution of a restricted environment. *Sedimentology*, *55*, 557–578.

Brown, E. T., Callonnec, L. L., & German, C. R. (2000). Geochemical cycling of redox-sensitive metals in sediments from Lake Malawi: A diagnostic paleotracer for episodic changes in mixing depth. *Geochimica et Cosmochimica Acta*, *64*, 3515–3523.

Chen, Y., Courtillot, V., Cogne, J. P., Besse, J., Yang, Z., & Enkin, R. (1993). The configuration of Asia prior to the collision of India: Cretaceous paleomagnetic constraints. *Journal of Geophysical Research*, *98*, 21927–21941.

Cogne, J. P., Kravchinsky, V. A., Halim, N., & Hankard, F. (2005). Late Jurassic–Early Cretaceous closure of the Mongol-Okhotsk Ocean demonstrated by new Mesozoic palaeomagnetic results from the Trans-Baikal area (SE Siberia). *Geophysics Journal of International*, *163*, 813–832.

Cohen, A. S., Lezzar, K. E., Cole, J., Dettman, D., Ellis, G. S., Gonneea, M. E., … Zilifi, D. (2006). Late Holocene linkages between decade–century scale climate variability and productivity at Lake Tanganyika, Africa. *Journal of Paleolimnology*, *36*, 189–209. https://doi.org/10.1007/s10933-006-9004-y.

Dean, W. E., & Megard, R. O. (1993). Environment of deposition of $CaCO_3$ in Elk Lake, Minnesota. In J. P. Bradbury & W. E. Dean (Eds.), *Elk Lake, Minnesota: Evidence for rapid climate change in the North-Central United States:* Geological Society of America Special Paper 276, 135–157, Boulder, Colorado.

Del Cura, M. A. G., Calvo, J. P., Ordonez, S., Jones, B. F., & Canaveras, J. C. (2001). Petrographic and geochemical evidence for the formation of primary, bacterially induced lacustrine dolomite: La Roda 'white earth' (Pliocene, central Spain). *Sedimentology*, *48*, 897–915.

Donskaya, T. V., Gladkochub, D. P., Mazukabzov, A. M., & Ivanov, A. V. (2013). Late Paleozoic–Mesozoic subduction-related magmatism at the southern margin of the Siberian continent and the 150 million-year history of the Mongol–Okhotsk Ocean. *Journal of Asian Earth Sciences*, *62*, 79–97.

Ehiro, M., Zakharov, Y. D., & Minjin, C. (2006). Early Triassic (Olenekian) ammonoids from Khentey Province, Mongolia, and their paleobiogeographic significance. *Bulletin of Tohoku University Museum*, *5*, 83–97.

Emeis, K. C., & Weissert, H. (2009). Tethyan–Mediterranean organic carbon-rich sediments from Mesozoic black shales to sapropels. *Sedimentology*, *56*, 247–266.

Enters, D., Kirilova, E., Lotter, A. F., Luecke, A., Parplies, J., Jahns, S., … Zolitschka, B. (2010). Climate change and human impact at Sacrower See (NE Germany) during the past 13,000 years: A geochemical record. *Journal of Paleolimnology*, *43*, 719–737.

Erba, E., Duncan, R. A., Bottini, C., Tiraboschi, D., Weissert, H., Jenkyns, H. C., & Malinverno, A. (2015). Environmental consequences of Ontong java plateau and Kerguelen plateau volcanism. In C. R. Neal, W. W. Sager, T. Sano, & E. Erba (Eds.), *The origin, evolution, and environmental impact of oceanic large igneous provinces* Geological Society of America Special Paper 511, 1–24, Boulder, Colorado.

Erdentsogt, B., Lee, I., Bat-Erdene, D., & Jargal, L. (2009). Mongolian coal-bearing basins: Geological settings, coal characteristics, distribution, and resources. *International Journal of Coal Geology*, *80*, 87–104.

Follmi, K. B. (2012). Early Cretaceous life, climate and anoxia. *Cretaceous Research*, *35*, 230–257.

Gorham, E., Dean, W. E., & Sanger, J. E. (1982). The chemical composition of lakes in the north-central United States. *Limnology and Oceanography*, *28*, 287–301.

Gradstein, F. M., Ogg, J. G., Schmitz, M., & Ogg, G. (2012). The geologic time scale 2012. Oxford, UK: Elsevier.

Gradzinski, R., Kielan-Jaworowska, Z., & Maryanska, T. (1977). Upper Cretaceous Djadokhta, Barun Goyot and Nemegt formations of Mongolia. *Acta Geologica Polonica*, *27*, 281–317.

Graham, S. A., Hendrix, M. S., Barsbold, R., Badamgarav, D., Sjostrom, D., Kirschner, W., & Mcintosh, J. S. (1997). Stratigraphic occurrence, paleoenvironment, and description of the oldest known dinosaur (Late Jurassic) from Mongolia. *Palaois*, *12*, 292–297.

Graham, S. A., Hendrix, M. S., Johnson, C. L., Badamgarav, D., Badarch, G., Amory, J., … Hacker, B. R. (2001). Sedimentary record and tectonic implications of late Mesozoic rifting, southeast Mongolia. *Geological Society of America, Bulletin*, *113*, 1560–1579.

Gubin, Y. M., & Sinitza, S. M. (1993). Triassic terrestrial tetrapods of Mongolia and the geological structure of the Sain-Sar-Bulak locality. In S. G. Lucas & M. Morales (Eds.), *The Nonmarine Triassic* (Vol. *3*, pp. 169–170). New Mexico, USA: New Mexico Museum of Natural History and Science, Bulletin.

Halim, N., Kravchinsky, V., Gilder, S., Cogne, J. P., Alexyutin, M., Sorokin, A., … Chen, Y. (1998). A palaeomagnetic study from the Mongol–Okhotsk region: Rotated Early Cretaceous volcanics and remagnetized Mesozoic sediments. *Earth and Planetary Science Letters*, *159*, 133–145.

Hankard, F., Cogne, J. P., & Kravchinsky, V. (2005). A new Late Cretaceous paleomagnetic pole for the west of Amuria block (Khurmen Uul, Mongolia). *Earth Planetary Science Letters*, *236*, 359–373.

Hasebe, N., Tamura, A., & Arai, S. (2013). Zeta equivalent fission-track dating using LA-ICP-MS and examples with simultaneous U–Pb dating. *Island Arc*, *22*, 280–291.

Hasegawa, H., Tada, R., Ichinnorov, N., & Minjin, C. (2009). Lithostratigraphy and depositional environments of the Upper Cretaceous Djadokhta Formation, Ulan Nuur basin, southern Mongolia, and its paleoclimatic implication. *Journal of Asian Earth Sciences*, *35*, 13–26.

Hasegawa, H., Tada, R., Jiang, X., Suganuma, Y., Imsamut, S., Charusiri, P., … Khand, Y. (2012). Drastic shrinking of the Hadley circulation during the mid-Cretaceous Supergreenhouse. *Climate of the Past*, *8*, 1323–1337.

Hautevelle, Y., Michels, R., Malartre, F., Elie, M., & Trouiller, A. (2007). Tracing of variabilities within a geological barrier by molecular organic geochemistry. Case of the Callovo-Oxfordian sedimentary series in the East of the Paris Basin (France). *Applied Geochemistry*, *22*, 736–759.

Hendrix, M. S., Graham, S. A., Amory, J. Y., & Badarch, G. (1996). Noyon Uul (King Mountain syncline), southern Mongolia: Early Mesozoic sedimentary record of the tectonic amalgamation of central Asia. *Geological Society of America, Bulletin*, *108*, 1256–1274.

Ichinnorov, N. (1998). New palynomorph assemblage from the Lower Cretaceous sediments of Bayan-Erkhet, Mongolia. *Mongolian Geoscientist*, *9*, 18–25.

Ichinnorov, N. (2005). Palynostratigraphic results of Shinekhudag and Khukhteeg Formations, Eastern Mongolia. *Mongolian Geoscientist*, *27*, 12–14.

Ichinnorov, N., & Hofman, C. C. (2012). Palynology studies of the Matad area (Tamsag Basin) Southeastern Mongolia. *Geology Sudlal*, *21*, 63–77.

Ichinnorov, N., Purevsuren, S., & Buyantegsh, B. (2008). Preliminary result of palynological study of the Khootiin Khotgor locality. *MUST, Geology Journal*, *19*, 81–86 (in Mongolian).

Itaya, T., Nagao, K., Inoue, K., Honjou, Y., Okada, T., & Ogata, A. (1991). Argon isotope analysis by a newly developed mass spectrometric system for K–Ar dating. *Mineralogical Journal*, *15*, 203–221.

Iwano, H., Orihashi, Y., Hirata, T., Ogasawara, M., Danhara, T., Horie, K., … Yamamoto, K. (2013). An inter-laboratory evaluation of OD-3 zircon for use as a secondary U–Pb dating standard. *Island Arc*, *22*, 382–394.

Jerzykiewicz, T., & Russell, D. A. (1991). Late Mesozoic stratigraphy and vertebrates of the Gobi Basin. *Cretaceous Research*, *12*, 345–377.

Johnson, C. L. (2004). Polyphase evolution of the East Gobi basin: Sedimentary and structural records of Mesozoic-Cenozoic intraplate deformation in Mongolia. *Basin Research*, *16*, 79–99.

Johnson, C. L., & Graham, S. A. (2004). Sedimentology and reservoir architecture of a synrift lacustrine delta, southeastern Mongolia. *Journal of Sedimentary Research*, *74*, 770–785.

Johnson, C. L., Greene, T. J., Zinniker, D. A., Moldowan, M. J., Hendrix, M. S., & Carroll, A. R. (2003). Geochemical characteristics and correlation of oil and nonmarine source rocks from Mongolia. *American Association of Petroleum Geologists, Bulletin*, *87*, 817–846.

Keller, A. M. D., & Hendrix, M. S. (1997). Paleoclimatologic analysis of a Late Jurassic petrified forest, southeastern Mongolia. *Palaios*, *12*, 280–289.

Khand, Y., Badamgarav, D., Ariunchimeg, Y., & Barsbold, R. (2000). Cretaceous system in Mongolia and its depositional environments. In H. Okada & N. J. Mateer (Eds.), *Cretaceous environments of Asia* (Vol. *17*, pp. 49–79). Amsterdam, Netherlands: Developments in Palaeontology and Stratigraphy: Elsevier.

Kouchi, Y., Orihashi, Y., Obata, H., Fujimoto, T., Haruta, Y., & Yamamoto, K. (2015). Zircon U- Pb dating by 213 nm Nd: YAG laser ablation inductively coupled plasma mass spectrometry: Optimization of the analytical condition to use NIST SRM 610 for Pb/U fractionation correction. *Chikyukagaku (Geochemistry)*, *49*, 19–35 (in Japanese with English abstract).

Krassilov, V. (1982). Early Cretaceous flora of Mongolia. *Palaeontographica B*, *181*, 1–43.

Kravchinsky, V. A., Cogne, J.-P., Harbert, W. P., & Kuzmin, M. I. (2002). Evolution of the Mongol–Okhotsk Ocean as constrained by new palaeomagnetic data from the Mongol–Okhotsk suture zone, Siberia. *Geophysics Journal of International*, *148*, 34–57.

Lamb, M. A., Badarch, G., Navratil, T., & Poier, R. (2008). Structural and geochronologic data from the Shin Jinst area, eastern Gobi Altai, Mongolia: Implications for Phanerozoic intracontinental deformation in Asia. *Tectonophysics*, *451*, 312–330.

Last, W. M. (1991). Lacustrine dolomite – an overview of modern, Holocene, and Pleistocene occurrences. *Earth-Science Reviews*, *27*, 221–263.

Li, G., Ando, H., Hasegawa, H., Yamamoto, M., Hasegawa, T., Ohta, T., … Ichinnorov, N. (2014). Confirmation of a Middle Jurassic age for the Eedemt Formation in Dundgobi Province, southeast Mongolia: Constraints from the discovery of new spinicaudatans (clam shrimps). *Alcheringa*, *38*, 305–316.

Louis-Schmid, B., Rais, P., Schaeffer, P., Bernasconi, S. M., & Weissert, H. (2007). Plate tectonic trigger of changes in pCO_2 and climate in the Oxfordian (Late Jurassic): Carbon isotope and modeling evidence. *Earth Planetary Science Letters*, *258*, 44–60.

Luder, B., Kirchner, G., Luecke, A., & Zolitschka, B. (2006). Palaeoenvironmental reconstructions based on geochemical parameters from

annually laminated sediments of Sacrower See (northeastern Germany) since the 17th century. *Journal of Paleolimnology*, *35*, 897–912.
Ludwig, K. R. (2012). *Isoplot 3.75: A geochronological toolkit for microsoft excel*. Berkeley Geochronological Center Special Publication, 5, Berkeley, USA: Berkeley Geochronological Center.
Makulbekov, N. M., & Kurzanov, S. M. (1986). The biogeographical relationships of the late Cretaceous biota of Mongolia. In A. Y. Rozanov, et al. (-Eds.), Trudy (Vol. *29*, pp. 106–112), Moscow, Russia (In Russian).
Martinson, G. G. (1982). The upper Cretaceous mollusks of Mongolia. In L. A. Nevesskaya (Ed.), *The Joint Soviet–Mongolian Palaeontological Expedition* (Vol. *17*, pp. 5–76), Moscow, Russia (in Russian).
Martinson, G. G., & Shuvalov, V. F. (1973). Stratigraphical division of the Upper Jurassic and Lower Cretaceous of South-east Mongolia. *Izvestiya Akademii Nauk SSSR, Seriya Geologicheskaya*, *10*, 139–143 (in Russian).
Meng, Q. R. (2003). What drove late Mesozoic extension of the northern China–Mongolia tract? *Tectonophysics*, *369*, 155–174.
Meng, Q. R., Hu, J. M., Jin, J. Q., Zhang, Z. Y., & Xu, Z. D. F. (2003). Tectonics of the late Mesozoic wide extensional basin system in the China-Mongolia border region. *Basin Research*, *15*, 397–415.
Metelkin, D. V., Vernikovsky, V. A., Kazansky, A. Y., & Wingate, M. T. D. (2010). Late Mesozoic tectonics of Central Asia based on paleomagnetic evidence. *Gondwana Research*, *18*, 400–419.
Nessov, L. A. (1985). Data on Late Mesozoic turtles from the USSR. *Studia Palaeocheloniologica*, *1*, 215–223.
Nichols, D. J., Matsukawa, M., & Ito, M. (2006). Palynology and age of some Cretaceous nonmarine deposits in Mongolia and China. *Cretaceous Research*, *27*, 241–251.
Nozaki, T., Kato, Y., & Suzuki, K. (2013). Late Jurassic ocean anoxic event: Evidence from voluminous sulphide deposition and preservation in the Panthalassa. *Scientific Reports*, *3*, 1889. https://doi.org/10.1038/srep01889.
Ojala, A. E. K., Francus, P., Zolitschka, B., Besonen, M., & Lamoureux, S. F. (2012). Characteristics of sedimentary varve chronologies – A review. *Quaternary Science Reviews*, *43*, 45–60.
O'Sullivan, P. E. (1983). Annually-laminated sediments and the study of Quaternary environmental changes – A review. *Quaternary Science Reviews*, *1*, 245–313.
Powell, T. G. (1986). Petroleum geochemistry and depositional setting of lacustrine source rocks. *Marine and Petroleum Geology*, *3*, 200–219.
Pruner, P. (1992). Palaeomagnetism and palaeogeography of Mongolia from the Carboniferous to the Cretaceous - final report. *Physics of the Earth and Planetary Interiors*, *70*, 169–177.
Rais, P., Louis-Schmid, B., Bernasconi, S. M., & Weissert, H. (2007). Palaeoceanographic and palaeoclimatic reorganization around the Middle-Late Jurassic transition. *Palaeogeography, Palaeoclimatology, Palaeoecology*, *251*, 527–546.
Remy, R. R., & Ferrell, R. E. (1989). Distribution and origin of analcime in marginal lacustrine mudstone of the Green River Formation, South-Central Uinta Basin, Utah. *Clays and Clay Minerals*, *37*, 419–432.
Sha, J. G. (2007). Cretaceous stratigraphy of northeast China: Non-marine and marine correlation. *Cretaceous Research*, *28*, 146–170.
Shanahan, T., Overpeck, J. T., Beck, J. W., Wheeler, C. W., Peck, J. A., King, J. W., & Scholzet, C. A. (2008). The formation of biogeochemical laminations in Lake Bosumtwi, Ghana, and their usefulness as indicators of past environmental changes. *Journal of Paleolimnology*, *40*, 339–355. https://doi.org/10.1007/s10933-007-9164-4.
Shuvalov, V. F. (1975). Stratigraphy of Mesozoic deposits of central Mongolia. In N. S. Zaitsev, B. Luwsandansan, G. G. Martinson, V. V. Menner, T. G. Pavlova, A. V. Peive, et al. (Eds.), *Stratigraphy of Mesozoic deposits of Mongolia* (Vol. *13*, pp. 50–112). Transactions of the Joint Soviet-Mongolia Scientific Research Geological Expedition, Moscow, Russia.
Shuvalov, V. F. (2000). The Cretaceous stratigraphy and paleobiogeography of Mongolia. In M. J. Benton, M. A. Shishkin, E. N. Kurochkin, & D. M. Unwin (Eds.), *The age of dinosaurs in Russia and Mongolia* (pp. 256–278). Cambridge, UK: Cambridge University Press.
Sladen, C., & Traynor, J. J. (2000). Lakes during the evolution of Mongolia: Lake basins through space and time. *AAPG Studies in Geology*, *46*, 35–57.
Sochava, A. V. (1975). Stratigraphy and lithology of the Upper Cretaceous deposits of South Mongolia. *Trudy Sovmestnaya Sovetsko-Mongol'skaya Paleontologiskoi Ekspeditsii*, *13*, 113–182 (in Russian).
Sochava, A. V. (1977). The Early Cretaceous stromatolites of Mongolia. *Trudy Sovmestnaya Sovetsko-Mongol'skaya Paleontologiskoi Ekspeditsii*, *14*, 145–160 (in Russian).
Sodov, J. (1980). New species of *Hielungia* and *Pityospermum* from Mesozoic sediments of the South-Eastern Mongolia. *Paleontological Journal*, *4*, 131–133 (in Russian).
Sodov, J. (1985). About age of Mesozoic sediments of Khootiin Khotgor Valley by paleobatonic data. *Geological Problem of Mongolia*, *9*, 177–184 (in Russian).
Sodov, J. (1990). Stratigraphic and paleobatonic characteristics of Jurassic sediments of Mongolia. In *Geology and mineral resources of Mongolian People's Republic* (pp. 163–167). Moscow: Nedra publication (in Russian).
Steiger, R. H., & Jager, E. (1977). Subcommission on geochronology: Convention on the use of decay constants in geo- and cosmochronology. *Earth and Planetary Science Letters*, *36*, 359–362.
Traynor, J. J., & Sladen, C. (1995). Tectonic and stratigraphic evolution of the Mongolian People's Republic and its influence on hydrocarbon geology and potential. *Marine and Petroleum Geology*, *12*, 35–52.
Van Itterbeeck, J., Horne, D. J., Bultynck, P., & Vandenberghe, N. (2005). Stratigraphy and palaeoenvironment of the dinosaur-bearing Upper Cretaceous Iren Dabasu Formation, Inner Mongolia, People's Republic of China. *Cretaceous Research*, *26*, 699–725.
Vitek, N. S., & Danilov, I. G. (2014). Soft-shelled turtles (Trionychidae) from the Cenomanian of Uzbekistan. *Cretaceous Research*, *49*, 1–12.
Watson, M. P., Hayward, A. B., Parkinson, D. N., & Zhang, Z. M. (1987). Plate tectonic history, basin development and petroleum source rock deposition onshore China. *Marine and Petroleum Geology*, *4*, 205–225.
Weissert, H. (2011). Mesozoic pelagic sediments: Archives for ocean and climate history during green-house conditions. In H. Hüneke & T. Mulder (Eds.), Developments in sedimentology (Vol. *63*, pp. 765–792), Amsterdam, The Netherlands.
Yamamoto, M., Bat-Erdene, D., Ulziikhishig, P., Enomoto, M., Kajiwara, Y., Takeda, N., … Nakajima, T. (1993). Preliminary report on geochemistry of Lower Cretaceous Dsunbayan oil shales, eastern Mongolia. *Bulletin of the Geological Survey of Japan*, *44*, 685–691.
Yamamoto, M., Bat-Erdene, D., Ulziikhishig, P., Watanabe, Y., Imai, N., Kajiwara, Y., … Nakajima, T. (1998). Organic geochemistry and palynology of Lower Cretaceous Zuunbayan oil shales. *Bulletin of Geological Survey of Japan*, *49*, 257–274.
Yang, Y. T., Guo, Z. X., Song, C. C., Li, X. B., & He, S. (2015). A short-lived but significant Mongol–Okhotsk collisional orogeny in latest Jurassic–earliest Cretaceous. *Gondwana Research*, *28*, 1096–1116. https://doi.org/10.1016/j.gr.2014.09.010.
Yuan, F., & Chen, P. (2005). Early Cretaceous Crustacea (Ostracoda, Conchostraca) from the Shine-Khudug Formation of SE Mongolia. *Acta Palaeontologica Sinica*, *44*, 25–35. (in Chinese, English abstract).
Zhang, H., Wang, M. X., & Liu, X. W. (2008). Constraints on the upper boundary age of the Tiaojishan formation volcanic rocks in West Liaoning-North Hebei by LA-ICP-MS dating. *Chinese Science Bulletin*, *53*, 3574–3584.
Zhao, X., Coe, R. S., Zhou, Y., Wu, H., & Wang, J. (1990). New paleomagnetic results from northern China: Collision and suturing with Siberia and Kazakhstan. *Tectonophysics*, *181*, 43–81.
Zolitschka, B., Francus, P., Ojala, A. E. K., & Schimmelmann, A. (2015). Varves in lake sediments: A review. *Quaternary Science Reviews*, *117*, 1–41.
Zorin, Y. A. (1999). Geodynamics of the western part of the Mongolia-Okhotsk collisional belt, Trans-Baikal region (Russia) and Mongolia. *Tectonophysics*, *306*, 33–56.

How to cite this article: Hasegawa H, Ando H, Hasebe N, et al. Depositional ages and characteristics of Middle–Upper Jurassic and Lower Cretaceous lacustrine deposits in southeastern Mongolia. *Island Arc*. 2018;e12243. https://doi.org/10.1111/iar.12243

Graphical abstract

Depositional ages and characteristics of Middle–Upper Jurassic and Lower Cretaceous lacustrine deposits in southeastern Mongolia

Hitoshi Hasegawa, Hisao Ando, Noriko Hasebe, Niiden Ichinnorov, Tohru Ohta, Takashi Hasegawa, Masanobu Yamamoto, Gang Li, Bat-Orshikh Erdenetsogt, Ulrich Heimhofer, Takayuki Murata, Hironori Shinya, G. Enerel, G. Oyunjargal, O. Munkhtsetseg, Noriyuki Suzuki, Tomohisa Irino, and Koshi Yamamoto

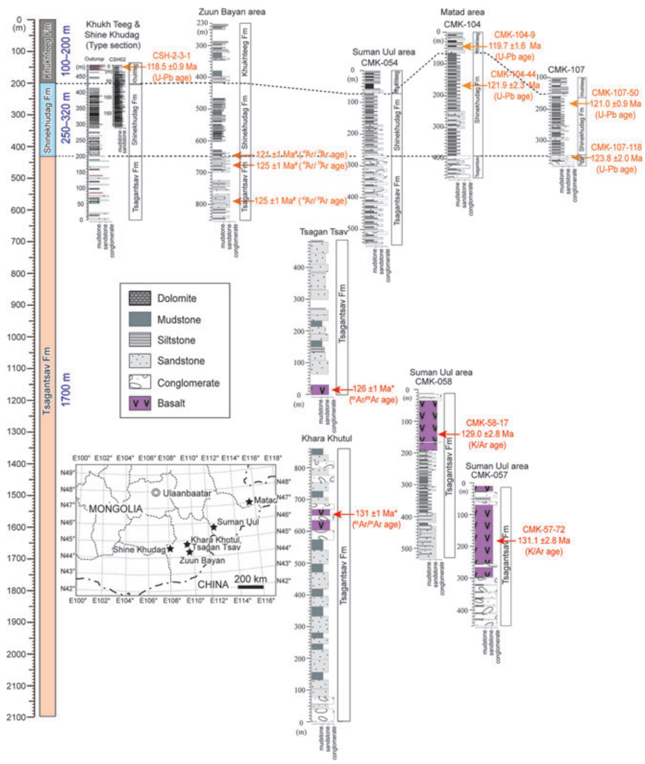

The present study aims at establishing depositional ages and characteristics of the Jurassic and Cretaceous lacustrine deposits in Mongolia. Based on radiometric age dating, the Shinekhudag Formation was deposited between (123.8 ±2.0) Ma and (118.5 ±0.9) Ma of early Aptian, and the Eedemt Formation was deposited at around 165–158 Ma of Callovian–Oxfordian. Although basin tectonics may have affected the deposition of these lacustrine oil shales, enhanced precipitation within a humid climatic setting during the early Aptian and the Callovian–Oxfordian times is more likely to be a key factor of the widespread occurrence of lacustrine environments in southeast Mongolia.

WILEY Island Arc

RESEARCH ARTICLE

Depositional ages and characteristics of Middle–Upper Jurassic and Lower Cretaceous lacustrine deposits in southeastern Mongolia

Hitoshi Hasegawa, Hisao Ando, Noriko Hasebe, Niiden Ichinnorov, Tohru Ohta, Takashi Hasegawa, Masanobu Yamamoto, Gang Li, Bat-Orshikh Erdenetsogt, Ulrich Heimhofer, Takayuki Murata, Hironori Shinya, G. Enerel, G. Oyunjargal, O. Munkhtsetseg, Noriyuki Suzuki, Tomohisa Irino, Koshi Yamamoto

モンゴル南東部には下部白亜系湖成オイルシェールが広く分布する．最近の研究により，その年代は白亜紀前期だけではなく，ジュラ紀中期も含む可能性が示されている．本研究は，モンゴルのジュラ系および白亜系湖成層の堆積年代と特徴を解明することを目的とする．下部白亜系シネフダグ層および中部ジュラ系エーデムト層は，共に頁岩と苦灰岩の互層を主体とする．頁岩は高水位期に，苦灰岩は低水位期に堆積し，その互層は降水量変動に伴う湖水位変動を反映している．介在する凝灰岩の U-Pb 年代により，シネフダグ層は123.8 ±2.0 Ma から118.5 ±0.9 Ma のアプチアン期前期に，エーデムト層は約165-158 Maのカロビアン-オックスフォーディアンに堆積した．シネフダグ層の頁岩中には藻類起源有機物と粘土鉱物の互層からなるマイクロラミナが見られ，ラミナの平均層厚と平均堆積速度(4.7 ±2.6 cm/ky~10.0 ±7.6 cm/ky)から，ラミナは年縞であると解釈された．モンゴル南部の湖成層の堆積は，内陸盆地のテクトニクス活動に加え，アプチアン期前期とカロビアン-オックスフォーディアンにおいて湿潤気候が卓越したことが関係していたと考えられる．